

Chemical and physical characterization of traffic particles in four different highway environments in the Helsinki metropolitan area

Joonas Enroth^{1,2}, Sanna Saarikoski³, Jarkko Niemi^{4,5}, Anu Kousa⁴, Irena Ježek⁶, Griša Močnik^{6,7}, Samara Carbone^{3,9}, Heino Kuuluvainen⁸, Topi Rönkkö⁸, Risto Hillamo³, and Liisa Pirjola^{1,2,*}

[1] {Metropolia University of Applied Sciences, Department of Technology, Helsinki, Finland}

[2] {University of Helsinki, Department of Physics, Helsinki, Finland}

[3] {Finnish Meteorological Institute, Atmospheric Composition Research, Helsinki, Finland}

[4] {Helsinki Region Environmental Services Authority HSY, Helsinki, Finland}

[5] {University of Helsinki, Department of Environmental Sciences, Helsinki, Finland}

[6] {Aerosol d.o.o., Ljubljana, Slovenia}

[7] {Jožef Stefan Institute, Ljubljana, Slovenia}

[8] {Tampere University of Technology, Department of Physics, Tampere, Finland}

[9] {now at University of São Paulo, Department of Applied Physics, São Paulo, Brazil}

*Correspondence to: L. Pirjola (liisa.pirjola@metropolia.fi, liisa.pirjola@helsinki.fi)

Abstract

Traffic related pollution is a major concern in urban areas due to its deleterious effects on human health. The characteristics of the traffic emissions on four highway environments in the Helsinki metropolitan area were measured with a mobile laboratory, equipped with state-of-the-art instrumentation. Concentration gradients were observed for all traffic related pollutants, particle number (CN), particulate mass PM_{10} , black carbon (BC), organics and nitrogen oxides (NO and NO_2). Flow dynamics in different environments appeared to be an important factor for the dilution of the pollutants. For example, the half-decay distances for the traffic-related CN concentrations varied from 8 m to 83 m at different sites. The PM_{10} emissions from traffic mostly consisted of organics and BC. At the most open site, the ratio of organics to BC increased with the distance to the highway indicating condensation of volatile and semi-volatile organics on BC particles. This condensed organics was shown to be hydrocarbons as the fraction of hydrocarbon fragments in organics increased. Regarding the CN size distributions, particle growth during the dilution was not observed, however, the mass size distributions measured with a soot particle aerosol mass spectrometer (SP-AMS), showed a visible shift of the mode, detected at ~100 nm at the roadside, to a larger size when the distance to the roadside increased. The fleet average emission factors for the CN appeared to be lower and for the NO_2 higher than ten years ago. The reason is likely the increased fraction of light duty (LD) diesel vehicles in the past ten years. The fraction of heavy duty traffic, although constituting less than 10 % of the total traffic flow, was found to have a large impact on the emissions.

1 Introduction

Vehicle exhaust emissions constitute major sources of ultrafine particles (UFP, below 100 nm in diameter), black carbon (BC), organic carbon (OC), and NO_2 in urban environments (e.g. Pey et al., 2009; Morawska et al., 2008; Johansson et al., 2007; Lähde et al., 2012). Although during the last 15 years particle mass emissions have been significantly reduced due to the tightened emission regulations and improvements in vehicle technology, the number emissions of the smallest UFP particles (below 50 nm in diameter) have been observed to be significant (Rönkkö et al., 2013; Kumar et al., 2011). Besides the exhaust emissions participate in chemical and physical transformation processes in the atmosphere affecting urban visibility and global climate (IPCC, 2013), they have harmful health effects. Ultrafine particles can penetrate deep into the human pulmonary and blood-vascular systems increasing the risk to get asthma,

1 reduced lung function, cardiovascular disease, heart stroke, and cancer (Pope III and Dockery,
2 2006; Sioutas et al., 2005; Kettunen et al., 2007; Su et al., 2008; Alföldy et al., 2009). The
3 European Environment Agency has estimated that fine particles caused around 430 000
4 premature deaths in Europe and around 1900 in Finland in 2012 (EEA, 2015). Particularly,
5 people who live, work or attend school near major roads have an increased health risk.

6 During the last decade, pollutant gradients near highways have been extensively examined in
7 USA (Zhu et al., 2009; Clements et al., 2009; Hagler et al., 2009; Canagaratna et al., 2010;
8 Durant et al., 2010; Padró-Martínez et al., 2012; Massoli et al., 2012), in Canada (Beckerman
9 et al., 2008; Gilbert et al., 2007), in Australia (Gramotnev and Ristovski, 2004), in India
10 (Sharma et al., 2009), and in Finland (Pirjola et al., 2006, 2012; Lähde et al., 2014). Generally,
11 all of these studies showed that the pollutant concentrations were higher near highway than
12 further from the roadside, sharply decreasing to background levels within 300-500 m
13 downwind. However, Gilbert et al. (2007) discovered that the NO₂ concentration decreased
14 during the first 200 m distance from the edge of the highway but beyond 200 m downwind
15 started to increase indicating that other factors than the highway traffic influenced the increased
16 NO₂ concentration.

17 These studies showed that the concentration levels and gradient shapes of UFP and other
18 primary vehicular emissions near major roads depend in a complex way on many factors,
19 including meteorological conditions such as atmospheric stability, temperature, wind speed,
20 wind direction, and surface boundary layer height (Durant et al., 2010). Dilution is a very
21 crucial process, additionally it is accompanied by aerosol dynamics processes such as
22 nucleation, coagulation, condensation, evaporation and deposition (Kumar et al., 2011 and
23 references therein). In the diluting and cooling exhaust new particles are formed by
24 homogeneous nucleation during first milliseconds (Kittelson, 1998), after that they immediately
25 grow by condensation of condensable vapours. Low temperature favours nucleation and
26 condensation, whereas evaporation becomes important during high ambient temperature. On
27 the other hand, the majority of volatile organic compounds is emitted by vehicles during cold
28 starts (Weilenmann et al., 2009). Consequently, Padro-Martinez et al. (2012) report that the
29 gradient concentrations were much higher in winter than in summer, even 2-3 times higher as
30 observed by Pirjola et al. (2006). Also relative humidity might affect PM emissions by vehicles.
31 Typically, in the street scale (around 200 m from the roadside) coagulation is too slow to modify
32 particle size distribution. However, under inefficient dispersion conditions (wind speed < 1 m s⁻¹

¹) self- and inter-modal coagulation as well as condensation and evaporation might become important transforming the particle size distribution (Karl et al., 2016 and references therein). Besides dilution and aerosol dynamics, traffic fleet and flow rate (e.g. Zhu et al., 2009; Beckerman et al., 2008), background concentrations (Hagler et al., 2009), and atmospheric chemical and physical processes (Beckerman et al., 2008; Clements et al., 2009), all affect pollutant concentrations near the highways. Hagler et al. (2009) and Janhäll et al. (2015) found that local topography and land use, particularly noise barriers and roadside vegetation, can also be important factors determining the concentrations. In addition, the measurement results depend on sampling techniques and instruments used in studies.

Using single particle mass spectrometry the characteristics of vehicle emissions have been studied in the past decade on a dynamometer (e.g. Sodeman et al. 2005; Shields et al., 2007) and near a highway (e.g. Lee et al., 2015). Only a few of the published studies have investigated changes in exhaust particle chemical composition during dispersion. Clements et al. (2009) collected high-volume PM_{2.5} samples at 35 and 65 m distances from a major highway. They discovered that unlike the particle-bound elemental carbon (EC), organic carbon (OC) concentrations increased with the distance downwind. Instead, Durant et al. (2010) report a time-dependent decrease in the concentrations of particulate organics (Org) and hydrocarbon-like organic aerosol (HOA) up to 200-300 m downwind from a highway during morning hours. Massoli et al. (2012) present spatial-temporal gradients of the HOA and oxygenated organic aerosol (OOA) concentrations summed with the refractory BC (rBC) up to 500 m downwind from a highway. The sum of HOA and rBC mass concentration decreased with increasing distance whereas the sum of OOA and rBC was constant. The size distributions of organics and rBC pointed out that the fresh soot mode peaking at ~100 nm was slightly coated by the HOA material whereas the accumulation soot mode peaking at ~500 nm was heavily coated by the OOA material representing the background aerosol. The change in the chemical composition of traffic particles with the distance is caused by several reasons. The exhaust from the vehicles is hot when emitted but it cools quickly as it is mixed with ambient air. Cooling promotes the condensation of organic vapours on particles but as the exhaust is diluted with ambient air, concentration of gaseous semivolatile organic compounds (SVOCs) is reduced, leading to the evaporation of SVOCs from particles in order to maintain phase equilibrium (Robinson et al., 2010). So there is an ongoing competition between different processes in the emission plume;

new particle formation (nucleation), particle growth through condensation and coagulation, and decrease of particle mass by evaporation.

The objective of this study was to characterize the spatial variation of traffic-related air pollutants downwind from the four highways in the Helsinki metropolitan area during rush hours. The measurements were performed by a mobile laboratory van “Sniffer”, equipped with high time-resolution instrumentation. In addition to gaseous pollutants and particle number (CN), mass (PM) and size distribution, also the chemical composition of particles was measured. This study addresses the following questions: 1) how different environments affect dilution and concentration gradients, 2) how the properties of CN size distribution change as a function of distance and location, 3) how the chemical composition of the particles evolves as the pollutants move away from the road, and 4) what are the emission factors of the main pollutants in different environments. For the first time, pollutant gradients near several highways were investigated from various aspects by combining the physical measurements with the detailed chemical speciation by using the state-of-the art-instrumentation in a mobile measurement platform.

2 Experimental methods

2.1 Measurement sites and sampling strategy

Measurements of gaseous and particle pollutants were conducted at four different environments (Fig. 1) located next to three highways in the Helsinki metropolitan region in Finland. The highways Ring I and Ring III have two traffic lanes in each direction whereas the highway Itäväylä has three lanes in each direction. Each of the four measurement sites had a small dead end road with minimal traffic perpendicular to the highway. Measurements were performed by a mobile laboratory van Sniffer at four different locations: (1) driving within the traffic at the highway, (2) stationary measurements next to the highway, (3) approaching the highway by driving with an average speed of 6.6 ± 1.5 km/h along the small road (gradient measurements), and (4) background measurements for each environment at a suitable remote location approximately 500 m away from the highway. The gradient measurement periods and sites were selected so that wind was blowing from the direction of the highway to the measurement road. Because the concentration field varied spatially and temporally, the gradient measurements were performed up to eleven times per measurement occasion on each road. Depending on the

location and the length of the measurement road, a single approach took about two minutes. Some of the approaches suffered from cars passing close by, sudden gusts of wind or other disturbances, and these were excluded. A total of 89 successful approaches were recorded. The approaches were carried out so that sampling inlets were on upwind side in order to avoid Sniffer's own exhaust. Measurements were performed during rush hours, 7-10 am and 3-6 pm, on the period from 22 October to 6 November 2012.

During the stationary measurements by the highway the drivers manually calculated traffic flow for heavy duty (HD: trucks and buses) and light duty (LD: passenger cars and vans) vehicles during three minutes to each direction. The traffic counts, taken at each site, are summarized in Table 1.

For the northern wind, the gradient measurements were performed along Isovaarintie in Espoo, next to Ring III near Lake Pitkäjärvi (Fig. 1). The environment was very open, surrounded only by the fields. The maximum distance to Ring III from Isovaarintie was 250 m. The gradients were measured while approaching the Ring III from the end of Isovaarintie. The roadside measurements were taken from a stationary position 14 m from the Ring III. According to Finnish Transport Agency (2015) the annual mean traffic flow on the Ring III was around 40 000 vehicles per day, 4 000 of which were HD vehicles. The percentage of HD vehicles on this site, based on our manual three minute observations, was 8.7%. This was also the highest share of HD vehicles of the four investigated sites (Table 1). The speed limit on Ring III was 100 km/h.

For the southern wind, the gradient measurements were performed at Malmi from 11 m to a maximum of about 260 m from Ring I (Fig. 1). Malmi is a suburban semi-open area surrounded by few buildings and trees. There is another fairly busy road at the far end of the measurement road. The manual calculations showed that 4.8% of vehicles were HD vehicles (Table 1), whereas the annual mean traffic flow of Ring I at Malmi is around 55 000 vehicles per day of which about 3 300 are HD vehicles (Finnish Transport Agency, 2015). The speed limit on Ring I was 80 km/h. The Helsinki Region Environmental Services Authority (HSY) had an air quality monitoring station at Malmi, and the chemical composition and sources of PM₁ at this site have been discussed earlier in Aurela et al. (2015).

In the case of the southern wind, the measurements were also carried out at Itä-Pakila on Klaukkalantie next to Ring I (Fig. 1). Itä-Pakila is a fairly uniform area with tightly built small houses with gardens (allotment). The highway is separated from the residential area with a noise

1 barrier. Mostly it is a land barrier with a row of spruce trees planted on its top, the height being
2 around 5 m. Only at the westernmost part (~ 100 m from the gradient start) the barrier is around
3 2 m high wooden fence. At the location of the gradient measurements the wooden fence has an
4 opening for pedestrian traffic, and a pedestrian bridge crossing the highway (Fig. 1). In addition
5 to the roadside and gradient measurements, the pedestrian walkway behind the noise barrier
6 was also measured on each of the routes. At Itä-Pakila the maximum distance of the gradient
7 measurements was about 260 m from the highway. The roadside measurements were performed
8 on a bus stop next to Ring I (6 m from the roadside). The manual count of mean traffic flow on
9 Ring I next to Itä-Pakila was highest of the four investigated sites, about 5 900 LD and 160 HD
10 vehicles per hour. It was the highest also according to the authorities, which report 57 000
11 vehicles per day, 3 200 of which are HD vehicles (Finnish Transport Agency, 2015). The speed
12 was limited to 80 km/h.

13 For the northwestern wind, the gradient road used for highway Itäväylä was at Herttoniemi,
14 Helsinki (Fig. 1). The maximum distance to Itäväylä was 130 m. The Herttoniemi measurement
15 site is in a semi-industrial area, with a rough surface environment. At Herttoniemi most
16 measurements were performed as stationary measurements at the distances of 11 (roadside), 20,
17 30, 40, 50, 70, 100 and 130 m from Itäväylä. The mean traffic flow on Itäväylä is around 50 000
18 vehicles per day (Finnish Transport Agency, 2015), and the speed limit was 80 km/h. The
19 Herttoniemi site was partially chosen because it had already been used nine years ago in the
20 LIPIKA project (Pirjola et al., 2006), thus enabling the comparison of the results.

21 Typical to Finnish autumn weather, the temperature was around 0.8-4.7°C, relative humidity
22 77-89%, and wind speed around 3-5 m s⁻¹, monitored at the meteorological measurement site
23 at Ämmässuo (Fig. 1) by the HSY. The measurement altitude was 15 m so these values
24 represent regional air mass properties. A summary of the meteorological and traffic conditions
25 at each site is presented in Table 1.

26 **2.2 Instrumentation**

27 Measurements were performed with a mobile laboratory van “Sniffer” (VW LT35 diesel van)
28 described in detail in Pirjola et al. (2004, 2006, 2012, 2015). The inlets were positioned above
29 the van’s windshield, 2.4 m above the ground level. During the stationary measurements, the
30 engine was switched off and the data of the first three minutes was excluded. The list of the
31 instruments is given in Table S1 in the upplement and desribed shortly below.

Particle number concentrations and size distributions were measured with two ELPIs, (Electrical Low Pressure Impactor, Dekati Ltd.) (Keskinen et al., 1992) both equipped with a filter stage (Marjamäki et al., 2002). Furthermore, an additional stage designed to enhance the particle size resolution for nanoparticles was installed into one ELPI (Yli-Ojanperä et al., 2010). The particle size distribution was also measured with an EEPS (Engine Exhaust Particle Sizer, model 3090, TSI). The measurement ranges of the ELPIs and EEPS were 7 nm - 10 µm and 5.6 - 560 nm, respectively, and the time resolution of one second was fast enough to register dynamic changes in the traffic exhaust while driving. It should be noted that the ELPIs measure particle aerodynamic diameters while the EEPS measures particle electrical mobility diameter. The number concentration of particles larger than 2.5 nm was measured by a butanol CPC (3776, TSI) with a time resolution of one second.

To study particle volatility characteristics, a thermodenuder (TD; Rönkkö et al., 2011) was installed in front of the ELPI which did not have an additional stage. In the TD, the diluted sample was heated to 265 °C and after that, led into the denuder where the cooled inner wall was covered with activated carbon to collect evaporated compounds. The particle size distributions measured after the TD were corrected for particle losses (Heikkilä et al., 2009).

Black carbon (BC) in the PM₁ size fraction (using a cyclone) was measured with an Aethalometer (Magee Scientific Model AE33) with one second time resolution. Measurements at 880 nm were used for the reported BC concentrations. The data was compensated for the loading effect using Drinovec et al. (2015), compensation algorithm with ten seconds time resolution.

For this study the Sniffer was also equipped with a SP-AMS (Soot Particle Aerosol Mass Spectrometer, Onasch et al., 2012) to study particle chemistry. In the SP-AMS, an intracavity Nd:YAG laser vaporizer (1064 nm) is added into the High Resolution Time-of-Flight Aerosol Mass Spectrometer (HR-ToF-AMS, DeCarlo et al., 2006) in order to measure rBC and associated non-refractory particulate material (e.g. metals) in addition to the non-refractory species, sulfate (SO₄), nitrate (NO₃), ammonium (NH₄), chloride (Chl) and organics (Org). In this study the SP-AMS measured in mass spectrum (MS) mode with five seconds time resolution of which half of the time the chopper was open and half of the time closed. In addition to MS mode, unit mass resolution (UMR) particle Time-of-Flight (pToF) data was collected at Pitkäljärvi and Herttoniemi in order to obtain the mass size distributions for the chemical species. There was a PM₁ cyclone in front of the SP-AMS but the real measured size range of

the instrument is ~50–800 nm (Canagaratna et al., 2007). The SP-AMS data was analyzed using a standard AMS data analysis software (SQUIRREL v1.57 and PIKA v1.16) within Igor Pro 6 (Wavemetrics, Lake Oswego, OR) and for the elemental analysis of organics an Improved-Ambient method was used (Canagaratna et al., 2015). The mass concentrations from the SP-AMS data were calculated by using a collection efficiency of 0.5 (Canagaratna et al., 2007 and references therein). Default relative ionization efficiencies (RIE) were used for organics, inorganic species and rBC. RIEs for metals were taken from Carbone et al. (2015). Even though both the aethalometer and SP-AMS can measure BC, only the data from the aethalometer is used in this paper for the concentrations of BC. The reason for this was that the SP-AMS gave much (~70%) smaller concentrations for rBC than aethalometer for BC, likely due to the nonoptimal laser-to-particle beam vertical alignment previously discussed e.g. in Massoli et al. (2012). However, for the mass size distributions (Section 3.3.2) rBC from the SP-AMS is used as the aethalometer can not give BC concentration as a function of the particle size. The SP-AMS has been used previously in traffic related measurements in e.g. Massoli et al. (2012), Dallmann et al. (2014) and Pirjola et al. (2015).

In this study, the PM₁ concentration was estimated as the sum of the concentrations of BC, measured with the aethalometer, and organics and inorganics, measured with the SP-AMS.

Gaseous concentrations of CO₂ (model VA 3100, Horiba), CO (model CO12M, Environnement S.A.), and nitrogen oxides NO, NO₂ and NO_x (model APNA 360, Horiba) were monitored with a time resolution of one second. A weather station (model WAS425AH and model HMP45A, Vaisala) on the roof of the van at a height of 2.9 m above the ground level provided meteorological parameters. Additionally, a global positioning system (model GPS V, Garmin) recorded the van speed and position.

2.3 Data handling

For each site, the data was averaged as a function of distance from the curb of the road. The average values were calculated at 25 m intervals from 25 m up to 300 m from the curb, with the ending point depending on the location. Each distance i on the gradient represents the span from $i-12.5$ m to $i+12.5$ m. The distances were determined from the GPS data.

2.4 Emission factor calculations

Fleet emission factors were calculated for various pollutants using a method adapted from Yli-Tuomi et al. (2004). The fuel based emission factor indicates how much of a given pollutant is emitted per amount of fuel consumed. Since the modern car fleet has very high combustion efficiency, we can use an approximation where all carbon in the fuel is CO₂. Thus, the emission factor for pollutant X can be expressed as

$$EF_X = \frac{CMF_{CO_2} (X - X_{bg})}{CMF_{fuel} (CO_2 - CO_{2,bg})} \quad (1)$$

where X is the pollutant concentration, and X_{bg} and $CO_{2,bg}$ are the background concentrations. For the CO₂ production rate, we adopted a value provided by the VTT Technical Research Centre of Finland, $CMF_{CO_2}/CMF_{fuel} = 3,141 \text{ g (kg fuel)}^{-1}$, the same as used by Yli-Tuomi et al. (2004). Similar values were also reported in other papers like Ježek et al. (2015). In order to characterize the fleet more representatively, two minute averages were used in the emission factor calculations.

3 Results and discussion

3.1 Overview of the concentration gradients

Rapidly decreasing concentrations from the highway were observed for particle number and mass as well as gases on all four investigated locations. For each site, Table 2 summarizes the average concentrations over the entire measurement time while driving on a highway, while being parked at the roadside and at the background locations, along with the respective standard deviations. As in previous studies (Zhu et al., 2002, 2009; Pirjola et al., 2006; Massoli et al., 2012), the CN were found to drop rapidly and level out to slightly above background levels from 100 to 300 meters from the roadside. For example, the average CN on the highways varied from $(7.7 \pm 9.1) \times 10^4 \text{ cm}^{-3}$ at Herttoniemi to $(12.2 \pm 14.0) \times 10^4 \text{ cm}^{-3}$ at Pitkäjärvi, and the average background concentrations from $(7.1 \pm 2.0) \times 10^3 \text{ cm}^{-3}$ at Herttoniemi to $(10.9 \pm 2.0) \times 10^3 \text{ cm}^{-3}$ at Malmi. Considerable differences between the sites were found in the particle dilution. Figure 2 illustrates the normalized curves for the behavior of CN, PM₁, BC, organics, NO and NO₂, for each site when the background concentrations were first subtracted and then the concentrations were divided by the concentrations measured at the highway. Most rapid decrease was observed

1 at Itä-Pakila where a 50% reduction in the CN already occurred at a distance of 8 m from the
2 highway (Table S2). The exceptional dilution of pollutants at this site was obviously caused by
3 the noise barrier, since the gradient route went through a narrow gap between the barrier ends.
4 However, the measurements on the pedestrian walkway behind the noise barrier showed a large
5 variation in the CN concentration depending on the height and type of the noise barrier (Fig.
6 S1). The half-decay distance at Malmi was 83 m, and around 40 m at Herttoniemi and
7 Pitkäjärvi, based on the fitted curves in Fig. 2 (Table S2). According to the earlier studies
8 (Pirjola et al., 2006; Fig. 9), the average CN concentration downwind Itäväylä at Herttoniemi
9 was reduced to half of the concentration at the roadside at ~ 55 m from the middle of the
10 highway, i.e. ~ 40 m from the roadside.

11 Highest PM₁ concentrations measured at the highway were detected at Itä-Pakila (16.8 ± 14.6
12 $\mu\text{g m}^{-3}$) and Malmi ($17.1 \pm 17.2 \mu\text{g m}^{-3}$), and the lowest highway PM₁ was found at Pitkäjärvi
13 ($10.9 \pm 7.2 \mu\text{g m}^{-3}$) (Table 2). The highest roadside PM₁ concentration was as well measured at
14 Malmi ($12.5 \pm 5.7 \mu\text{g m}^{-3}$), and the lowest was found at Pitkäjärvi ($7.5 \pm 3.5 \mu\text{g m}^{-3}$) where the
15 background concentration was low as well. Rather similar reductions than for the CN can be
16 observed for the PM₁ concentrations. The strongest dilution occurred at Itä-Pakila where the
17 concentrations reduced to half of the highway concentration at 3 m at Itä-Pakila. The half-decay
18 distance was 75 m at Malmi, and 26-28- m at the other sites (Table S2).

19 The terrain dynamics of the different measurement sites appeared to be an important factor for
20 pollution dilution. The open environment of Pitkäjärvi produced smooth pollution gradients on
21 most runs while the more urbanized environments of Herttoniemi and Malmi had considerably
22 more variation present in their gradients. At Malmi, the presence of the second road at the end
23 of the measurement lane (at the distance of 175-200 m from Ring I) was also apparent in the
24 data, often resulting in a U-shaped pollution profile. The noise barrier lowered the pollutant
25 concentrations at Itä-Pakila considerably. Previous studies have found that sound barriers can
26 create constant local eddies in the wake of the sound barrier, resulting in a lower pollution zones
27 (Bowecker et al., 2007, Ning et al., 2010).

28 For the gaseous pollutants, the dilution rates were similar to those of the particle concentrations,
29 i.e. rapid decrease in the first tens of meters and leveling at 100-300 meters to the urban ambient
30 levels (Table 2). The exceptionally rapid dilution at Itä-Pakila was noted also with the NO
31 concentrations (Fig. 2). Consequently, the ratio of NO₂ to NO was higher than unity already at

50 m distance from the roadside whereas at least 100 m was needed at the other sites (Table S3).

Similarly, Massoli et al. (2012) did not observe a gradient for NO_2 , but found it to be dependent on the time of day. Thus they linked it to photochemical conversion, and concluded that NO_2 is not an efficient indicator of traffic pollutants on a short time scale. We observed rather similar behavior for NO_2 at Malmi, whereas a clear spatial NO_2 gradient near the highways could be observed at Itä-Pakila, Pitkäjärvi, and Herttoniemi. The observed gradient of NO_2 is likely explained by the difference in the vehicle fleet composition and the background NO_2 levels between New York and Helsinki. In Helsinki, the fraction of light duty diesel vehicles of the passenger cars is very high, 34.3 % (Official statistics of Finland, 2015), and thus there seems to be sufficient amount of NO_2 directly emitted from traffic to form an observable gradient. The sunrise and sunset during the measurement period coincided with the rush hours, thus making the analysis of photochemistry more difficult. NO did show time dependent behavior with higher concentrations present in the morning rush hour (Fig. S2). In the afternoon, it seems as though the emitted NO rapidly converted into NO_2 by O_3 oxidation, and as a result lower levels of NO were observed.

3.2 Particle number size distributions

Figure 3 shows the average number size distributions over all measured periods at different environments, recorded by the EEPS. Three modes can be observed, the nucleation mode peaked at ~10 nm, Aitken mode at ~30-40 nm and the soot mode at ~70-80 nm. Sometimes the nucleation mode had two peaks, one at ~10 nm and the other at 16-20 nm. The exact shape of the size distribution was observed to be dependent on the location. For example, the Aitken mode was largest at Itä-Pakila where the traffic flow was highest, consisting mostly of LD vehicles. Instead, the nucleation mode was highest at Pitkäjärvi where the traffic was not that busy but consisted more of HD vehicles.

Pirjola et al. (2006) observed particle growth in the nucleation mode with increasing distance from the highway during a previous winter campaign. Here, we did not observe significant growth of the mean diameter of the nucleation mode particles. When considering the whole size distribution in the size range of 5.6-560 nm, the average diameter (Table S4) grew by 1.7%, 2.1%, 22% and 17% at 100 m from the road for Herttoniemi, Malmi, Itä-Pakila and Pitkäjärvi, respectively, compared to the average diameter observed on the highway. It is plausible that

1 this growth mostly resulted from mixing with the background particles, that on average were
2 larger than the freshly emitted particles at all sites except at Herttoniemi (Table S4). During
3 dispersion the smallest particles decreased faster than the larger ones. For example, at 100 m
4 distance the particles in the size ranges from 6-30 nm, 30-60 nm, 60-150 nm and 150-500 nm
5 had decreased in their respective concentrations by 76, 68, 64 and 60% compared to the
6 concentrations measured on the highways.

7 Particle volatility was studied by two ELPs, one before and the other after the TD treatment.
8 Figure 4, presenting the results from Herttoniemi, indicate that particle volatility was size
9 dependent. The smallest particles (< 30 nm) were found to be highly volatile indicating that the
10 origin for these particles might be nucleation of sulfuric acid from fuel and lubricant oil sulfur
11 compounds along with volatile organic compounds (Arnold et al., 2012, Kittelson et al., 2008).
12 The existence of non-volatile cores (e.g. Rönkkö et al., 2007) in sub 30 nm particles could not
13 be estimated mainly because particles smaller than 7 nm cannot be measured by the ELPs.

14 The soot mode concentrations showed lowest reductions after the TD treatment. The size
15 distribution after the TD treatment peaked at around 70 nm by number and at ~200 nm by
16 volume (aerodynamic diameter) which coincides with the typical size of soot particles from
17 traffic emissions. The TD treatment reduced particle number and volume in 7-1000 nm size
18 range by 86% and 65% respectively, showing that most of the particle material was volatilized
19 at high temperatures.

20 **3.3 Chemical composition of traffic particles**

21 Particles at the highway and roadside comprised mostly of BC and organics (Table 2). The
22 contribution of BC to PM₁ (where PM₁ is the sum of chemical species measured with the SP-
23 AMS and aethalometer) was 54, 40, 28 and 41% at the highway at Herttoniemi, Malmi, Itä-
24 Pakila and Pitkäjärvi, respectively, with the corresponding contribution of organics being 41,
25 46, 54 and 51%. At the background locations, the particles were mainly made of organics and
26 sulfate (50 and 21% at Malmi, 52 and 17% at Itä-Pakila and 44% and 24% at Pitkäjärvi,
27 respectively) or organics and BC (60 and 26% at Herttoniemi). At Malmi and Itä-Pakila there
28 were also some nitrate and ammonium in the particles at the background location (11 and 8%
29 at Malmi and 13 and 9% at Itä-Pakila, respectively), and at Malmi the particles had a minor
30 fraction of chloride (3%). In addition to BC, organics and inorganic salts, particles were found
31 to contain trace amounts of metals. Metals will be discussed separately in Section 3.3.3.

1 An example of the chemical composition of PM₁ particles measured at different distances from
2 the road is presented in Fig. S3 at Pitkäjärvi. Only the major components are included in the
3 figure and therefore, e.g. chloride and the metals, are not shown. As seen from Fig. S3, the mass
4 fraction of BC decreased with the increasing distance from the road, whereas the fractions of
5 organics and inorganics (sulfate, ammonium and nitrate) increased, the contribution of
6 background aerosol becoming more predominant as moved further from the road.

7 Normalized dilution curves of organics and BC are presented in Fig. 2. For both organics and
8 BC the concentrations decreased fastest at the Itä-Pakila noise barrier site where these
9 concentrations dropped to half of those at the highway already at the roadside and nine meters
10 from the road, respectively (Table S2). Except at Itä-Pakila, the dilution curves for organics
11 were quite similar at all other sites. Regarding BC, the dilution curves had similar trends at
12 Herttoniemi and Pitkäjärvi, whereas at Malmi the concentration decreased up to 100 meters
13 from the road after which it remained at elevated level for the rest of the gradient. In general,
14 organics reached 50% reduction much earlier than BC except at Pitkäjärvi. The average half-
15 decay values over all sites for organics and BC were ~24 and 33 meters, respectively (Table
16 S2).

17 Figure 5a shows that the ratio of organics to BC varied from 0.58 to 1.34 at the highway. The
18 ratio was smallest at Herttoniemi and largest at Itä-Pakila. When moving away from the
19 highway, the evolution of the ratio was rather different at different sites. The ratio varied
20 significantly at Itä-Pakila, and therefore it is shown only with separate points in Fig. 5a. High
21 variation was probably due to the rapid decrease of traffic pollutants at Itä-Pakila (because of
22 noise barrier) and thus a high uncertainty in the calculation of organics to BC ratio as the ratio
23 was calculated only for traffic related particles after background subtraction. At Malmi the ratio
24 of organics to BC was clearly larger at 25 meters from the road whereas it was rather stable at
25 all other measurement points. At Herttoniemi and Pitkäjärvi the ratio of organics to BC
26 increased with the distance. At Herttoniemi the ratio increased slightly from the roadside up to
27 100 meters, whereas at Pitkäjärvi (open field site) the ratio increased, however not very
28 smoothly, all the way from the roadside to the last measured gradient distance 250 meters from
29 the road. At 250 meters from the road the ratio of organics to BC was already double what it
30 was at the highway at Pitkäjärvi. The increase of this ratio is assumed to be associated with the
31 condensation of volatile and semi-volatile organics on BC particles when hot exhaust aerosol
32 was mixed with ambient air and cooled. In general, during the dilution of exhaust aerosol, there

1 is a competition between particle formation, particle growth via condensation and coagulation,
2 and reduction of particle mass with evaporation. Chemical composition of organics and its size
3 distributions in traffic particles will be investigated in detail in next two sections.

4 For nitrate, sulfate and ammonium, no change in the concentrations with the distance was
5 observed (Fig. S4). This is expected as vehicles are not significant direct emitters of particulate
6 nitrate, and the use of ultra low sulfur diesel fuel results in very low emissions of particulate
7 sulfate. Similar results for sulfate, ammonium and nitrate have been shown e.g. in Durant et al.
8 (2010). However, at Herttoniemi and Pitkäjärvi the chloride concentrations were slightly larger
9 at the highway, roadside and near the road (≤ 50 m distance) than at the other measurement
10 points (Fig S4d). Chloride concentrations could be related to the lubricating oil, or in a small
11 part to the road salt used in Finland in wintertime.

12 3.3.1 Traffic-related organics

13 The composition of organic matter was investigated by dividing organic fragments based on
14 their elemental composition. In addition to carbon and hydrogen atoms, organic matter consists
15 of oxygen and, typically in small amounts, nitrogen and sulfur atoms. The chemical
16 composition of organics at the highway, roadside and background at all four sites are shown in
17 Fig. S5. Similar to the previous studies (e.g. Canagaratna et al., 2004; Chirico et al., 2011), most
18 of the organics consist of hydrocarbon fragments ($C_xH_y^+$) at all measurement locations. The
19 fraction of hydrocarbons decreased from highway to background, the portion of hydrocarbons
20 being on average 77, 70 and 53% at the highway, roadside and background, respectively. The
21 largest single fragments in $C_xH_y^+$ group were $C_4H_9^+$ (at m/z 57), $C_3H_7^+$ (at m/z 43), $C_4H_7^+$ (at
22 m/z 55) and $C_3H_5^+$ (at m/z 41; Fig. S5). Most of the other organics were made of oxygen-
23 containing fragments. Organic fragments with one oxygen atom ($C_xH_yO^+$) had slightly larger
24 fraction in organics than fragments with more than one oxygen atom ($C_xH_yO_z^+$, $z > 1$), especially
25 at the background sites. $C_xH_yO^+$ group had largest signal for $C_2H_3O^+$ (at m/z 43), CO^+ (at m/z
26 28) and CHO^+ (at m/z 29), fragments whereas $C_xH_yO_z^+$, $z > 1$ group consisted almost entirely
27 from CO_2^+ (at m/z 44). There was also an indication of nitrogen-containing organics ($C_xH_yN^+$)
28 in traffic particles, however, they were difficult to separate from neighboring peaks in the MS
29 as they constituted less than 1% of all organics.

30 When comparing the sites, the fractions of hydrocarbons and oxidized organics were similar at
31 all highway sites, whereas the fractions of oxidized organics at the roadside and background
32 were larger at Itä-Pakila than at Herttoniemi, Malmi and Pitkäjärvi. This was likely due to the

high contribution of long-range transport because elevated levels of nitrate, sulfate and ammonium were observed at all the measurement positions at Itä-Pakila site (Fig. S4). In line with the higher portion of oxygenated organic fragments, the ratios of oxygen to carbon (O:C) and organic matter to organic carbon (OM:OC) at the highway, roadside and background were larger at Itä-Pakila than at any other site (Fig. S5).

The fractions of hydrocarbons were smaller in this study than that in Dallman et al. (2014) measured in the San Francisco Bay area. They found that the family $C_xH_y^+$ contributed 91% of the measured organics signal, whereas the families $C_xH_yO^+$ and $C_xH_yO_z^+, z>1$ contributed less than 10%. However, they measured the vehicle emissions in a highway tunnel where the contribution of background organics was assumed to be smaller than in this study.

Concentration gradients for hydrocarbon and oxygen-containing organic fragments after the background subtraction are shown in Fig. 6a. It is clear that hydrocarbon concentrations decreased with the distance from the road but for oxidized fragments the concentrations depended less on the distance. At Herttoniemi, both oxidized fragments ($C_xH_yO^+$ and $C_xH_yO_z^+, z>1$) clearly fell off with the distance from the road, whereas at all the other sites the concentrations of the oxidized fragments were typically slightly larger at the highway. However, a decreasing trend from the road was not observed. The lack of any significant spatial gradient for oxidized fragments suggests that they mostly correspond to the aged background aerosol. Similarly, Canagaratna et al. (2010) observed a concentration gradient for hydrocarbon-like organic aerosol in Massachusetts, USA. Regarding the oxygenated organic aerosol they found an increase up to 150 meters from the road after which the OOA concentration decreased. It should be noted that in Fig. 6 some of the concentrations for the oxidized fragments are negative. That indicates that the measured concentrations were smaller than those measured at the background.

Organics in the engine exhaust particles originate from unburned fuel and lubricant oil as well as their partially oxidized products. Different processing technique for fuel and lubricant oil leads to large differences in their molecular weights and chemical structures. This results in divergent mass spectra (MS), e.g. diesel fuel MS has larger contribution of n-alkanes, whereas the lubricant oil MS is enriched in cycloalkanes and aromatics (Tobias et al. 2001). It has been suggested that lubricant oil dominates fuel as a source of primary organic aerosol under typical operating conditions of an engine (Tobias et al., 2001; Worton et al., 2014; Dallmann et al., 2014). However, separating organic species emitted from diesel and gasoline vehicles has

proved to be difficult. Varying levels of diesel trucks in vehicle fleet did not result in clear differences in the MS of organics measured with the SP-AMS (Dallmann et al., 2014).

The composition of organics was studied more carefully with the data collected at Pitkäjärvi. Pitkäjärvi was selected for the detailed investigation as the ratio of organics to BC changed with distance only at Pitkäjärvi, suggesting that the traffic particles underwent some atmospheric processing during the dilution. The average MS for rBC and organics measured at the highway, roadside, over all gradient sites, and background at Pitkäjärvi are shown in Fig. S6a. As already discussed, the MSs at the highway, roadside and gradient were dominated by hydrocarbon fragments and after the background subtraction hydrocarbon fragments from roadside and highway fell into straight line (Fig. S6b). The ratios of the hydrocarbon fragments were slightly different between gradient and roadside (Fig. S6c). Organics had more $C_3H_5^+$ fragment at m/z 41 during the gradient than at the roadside. Regarding the oxidized fragments, most of them were larger at the background than at the highway, roadside and gradient, shown by negative values in Fig. 6b, except CO^+ and CO_2^+ that were clearly higher near the road. Most distinctive negative oxidized fragment was $C_2H_3O^+$ at m/z 43, especially in the MS measured at the highway and roadside. When studying the behavior of $C_2H_3O^+$ with the distance more closely, it was found that its concentration was smaller only at the highway and roadside but after that it increased to a steady level and remained there for the rest of the gradient.

It was evident that the increase in organics relative to BC (Fig. 5a) was caused by the increase of hydrocarbons via condensation. By summing all hydrocarbon and oxidized fragments in the MS, the fraction of hydrocarbon fragments in organics increased when the distance to the road increased, especially after 150 meters from the road (Fig. 5b). In line with that the fraction of oxygen-containing organic fragments decreased with the distance, the descent being more pronounced for the organic fragments with one oxygen atom.

3.3.2 Mass size distributions

The evolution of particle chemistry during the dilution was also seen in the mass size distributions of chemical components. At Pitkäjärvi, the size distributions were measured only at the roadside and background (Fig. S7). It is clearly observable that a mode found at the roadside at ~100 nm disappeared almost totally when the size distributions were measured at the background location. This mode was dominated by organics (hydrocarbons) and rBC, similar to the previous studies measured by the AMS in traffic environments (e.g. Schneider et al., 2008; Canagaratna et al., 2010; Massoli et al., 2012; Lee et al., 2015). The mode at ~100

1 nm was found to be less volatile than the particles in the smaller and larger mode measured by
2 the two ELPIs and TD (Fig. 4), indicating that the material not evaporated in the TD was the
3 rBC core of the particles. A decrease of the mass in the TD in this mode was likely due to
4 hydrocarbon species. The second mode (at ~300-400 nm) was observed both at the roadside
5 and at the background (Fig. S7). At the background, this mode was mostly made of oxygen-
6 containing organic fragments and sulfate, whereas at the roadside there was also some rBC
7 present. The composition of the second mode was very similar to that found at Massoli et al.
8 (2012) for the particles upwind of Long Island Expressway. Based on the results from the SP-
9 AMS in the laser-only configuration they observed a mode at ~500 nm for rBC that was heavily
10 coated with organic material. However, they also suggested that the majority of the mode
11 peaking at ~500 nm consisted of organics and sulfate and that it was not associated with rBC
12 cores.

13 Similar to Pitkääjärvi, also at Herttoniemi there was a mode at ~100 nm (Fig. 7). In contrast to
14 the number size distributions (Fig. 3) the mass size distributions at Herttoniemi changed with
15 the distance from the road. For rBC, the peak of the mode was at 104 nm at the roadside,
16 whereas at 30 meters from the road the mode had become narrower and the maximum of the
17 mode had moved to 113 nm. At 40 meters from the road the peak of the rBC mode was found
18 already at 125 nm, and at the distance of 50 m it was at 148 nm. In this study, the dominant
19 mode for rBC was at a significantly smaller size than the mode obtained earlier for EC at the
20 same site at Herttoniemi, 65 meters from the road (Saarikoski et al., 2008). In the earlier study,
21 the maximum of the EC mode was between 300–500 nm. However, the used measurement
22 technique was quite different from the SP-AMS as the EC size distribution was measured by
23 using a small deposit area low pressure impactor with quartz substrates that were analyzed in
24 the laboratory with a thermal-optical transmittance method. Besides the measurement technique
25 and sampling time, also the meteorology as well as traffic volume could have been quite
26 different.

27 The shift of the ~100 nm mode is plausible due to the condensation of hydrocarbons on the rBC
28 particles in dilution. When studying the size distribution of hydrocarbons, it was observed that
29 at the roadside and at 30 meters from the road the maxima for hydrocarbons and rBC were at
30 nearly similar sizes but after that, especially at 40 meters from the road, hydrocarbons peaked
31 at the smaller size than rBC (Fig. S8). Also the relative concentration of hydrocarbons was
32 larger than that of rBC at 40 meters. This finding suggests that hydrocarbons were in the same

particles with the rBC, and most likely condensed on the surface of the rBC particles at 40 meters. However, at 50 meter distance the ratio of hydrocarbons to rBC was again similar to that at the roadside and 30 meters from the road. The behavior at a 50 m distance is difficult to explain, however, emissions from vehicles at the nearby street and parking lot probably disturbed our gradient measurements. The size distributions of rBC were obtained from the UMR pToF-data of the SP-AMS by using m/z 36 as a surrogate for rBC as C_3^+ at m/z 36 was the strongest carbon cluster signal in the rBC MS. Similarly, m/z 57 in UMR PToF-data was used as a surrogate for hydrocarbons. The size distribution traces m/z 36 and 57 were normalized to the mass concentrations of the corresponding species (rBC, $C_xH_y^+$) obtained from the high-resolution analysis.

3.3.3 Metals

The laser vaporizer used in the SP-AMS extends the range of chemical species detected by the AMS to include refractory species associated with rBC containing particles, such as metals and other elements (Onasch et al., 2012). Standard AMS has a tungsten vaporizer that is heated only up to 600 °C that is not enough for the fast vaporization of metals, however, some metals have been measured with the regular AMS without the laser (e.g. Salcedo et al., 2010, 2012). In this study, both laser and tungsten vaporizers were installed in the SP-AMS. The concentrations of metals were calculated from the signal values (in Hz) given by the SP-AMS by using the relative ionization efficiencies measured in the study of Carbone et al. (2015). Unfortunately, the size distributions were not obtained for the metals as the PToF data was saved only in UMR mode and the contributions of metals to the total signal measured at UMR m/z 's were very small.

Iron (Fe), vanadium (V), zinc (Zn) and aluminum (Al) were detected in the particles. At Herttoniemi, a clear gradient was found for Fe, Al and V whereas for Zn the concentration remained high until 50 meters from the road and dropped suddenly (Fig. 8a). At Pitkäjärvi, the concentrations of metals decreased slower than at Herttoniemi, and for all the metals there was a small increase at 75 meters from the road (Fig. 8b). That “bump” could not be explained. At Malmi and Itä-Pakila the concentration of metals did not change with the distance from the road (Fig. S9). That was probably due to the multiple sources of metals at those sites, which inhibited the observation of the concentration gradients from the highway.

In general, the concentration levels for metals were rather similar at Herttoniemi, Pitkäjärvi and Malmi, whereas at Itä-Pakila the concentration of vanadium was significantly elevated. Vanadium can be found in the particles from heavy oil combustion (Carbone et al., 2015) but

at Itä-Pakila there was no clear heavy oil combustion source nearby that could explain the elevated concentrations. Therefore vanadium was likely to be long-range transported together with sulfate and nitrate that had elevated concentrations at the same time at Itä-Pakila (Fig. S4). However, vanadium is used in catalysts (e.g. Blum et al., 2003) which might partly explain its concentration gradients in Fig. 8.

Aluminum and iron are were metals which can also originate from materials used at road surfaces, tires and brakes, whereas, zinc, phosphorus and magnesium are usually associated with lubricant oils (e.g. Pirjola et al., 2015; Rönkkö et al., 2014; Sodeman et al., 2006). Dallmann et al. (2014) detected zinc and phosphorus in the exhaust plumes of individual trucks by the SP-AMS. They noticed that the ratio of zinc and phosphorus to organics in the emission plume was consistent with typical weight fractions of additives often used in lubricant oils, and used that as an evidence that a large fraction of organics in gasoline exhaust originates from lubricating oil. In this study, phosphorus or magnesium was not detected in particles.

3.4 Emission factors

Fleet emission factors, based on the data while driving on the highways, were calculated for CN, PM₁, BC, organics, NO, NO₂ and NO_x. The average fleet emission factors for CN (particle diameter > 2.5 nm) were found to range from 4.9×10^{15} to 1.2×10^{16} # (kg fuel)⁻¹ (Table 3). The highest value was observed at Pitkäjärvi where the fraction of HD vehicles was highest (Table 1), and lowest at Herttoniemi where the HD fraction and also the total vehicle count were low. At Itä-Pakila, although the HD fraction was as small as at Herttoniemi, the total vehicle count was 51% greater and consequently, the average EF_{CN} was higher 6.5×10^{15} # (kg fuel)⁻¹. These results and Fig. S10 show that the fraction of HD vehicles has significant effect on the fleet emissions factor of CN.

In general, these results are slightly lower than the value of 9.3×10^{15} # (kg fuel)⁻¹ presented by Yli-Tuomi et al. (2004), who also performed measurements on the highways in the Helsinki metropolitan region. Our results are in agreement with the ones reported by Massoli et al. (2012) (mixed fleet: 5.3×10^{15} # (kg fuel)⁻¹), Westerdahl et al. (2008) (LD: 1.8×10^{15} and HD: 11×10^{15} # (kg fuel)⁻¹) and Ježek et al. (2015) (LD_{gasoline}: 1.95×10^{15} , LD_{diesel}: 4.4×10^{15} and HD_{diesel} (goods vehicles): 11.5×10^{15} # (kg fuel)⁻¹).

Contrary to the particle number emission factors, all the mass emission factors, EF_{PM₁}, EF_{BC} and EF_{Org}, were lowest at Pitkäjärvi. One should remember that there the nucleation mode was

very strong but it has only a small effect on the mass emissions. Additionally, the Aitken and soot mode concentrations were smaller than on the highways at the other sites (Fig. 3).

The EFs of NO found here (Table 3) were lower while the EFs of NO₂ were higher than the values of $10 \pm 19 \text{ g (kg fuel)}^{-1}$ for EF_{NO} and $2 \pm 5 \text{ g (kg fuel)}^{-1}$ for EF_{NO₂} reported by Yli-Tuomi et al. (2004). The increased EF_{NO₂}, with respect to the results of Yli-Tuomi et al. (2004), could be due to the higher direct NO₂ emissions of modern diesel cars as the fraction of light duty diesel vehicles of the passenger cars in Finland rose from 18.6 % to 34.3 % in the period between the measurements in years 2003-2015 (Official statistics of Finland, 2015). Carslaw et al. (2013) report that in London, the NO_x emissions reduced only from the gasoline fuelled vehicles over the past 15-20 years although the modern diesel vehicles were equipped with after-treatment systems, including SCR systems, designed to reduce NO_x emissions. Furthermore, the authors report that for the diesel passenger cars the relative amount of NO₂ was increased as the NO₂/NO_x ratio was 10-15% for Euro III and older type vehicles whereas it was 25-30% for Euro IV-V type vehicles. Ježek et al. (2015) observed reductions in the EF_{NO_x} for passenger cars and diesel heavy goods vehicles but no reduction for diesel passenger cars compared to the ten or more years old ones.

4. Summary and conclusions

The traffic emissions downwind from the four highways at the Helsinki metropolitan region in Finland were measured from 22th October to 6th November 2012 with the mobile measurement platform Sniffer. Measurements were conducted at four locations, within the traffic at the highway, at the roadside, at several distances from the highway (gradients), and at the background. As the pollutants dispersed away from the road, their concentration decreased mostly due to dilution and mixing with the background air. Concentration gradients were observed for the traffic related pollutants CN, PM₁, BC, organics, NO and NO₂, and for some metals. Furthermore, a change in the particle number and volume size distribution was noticed. The flow dynamics in the different environments appeared to be an important factor for the pollution dilution. The open environment of Pitkäjärvi produced smooth pollution gradients on the most runs while more complex urban environments of Herttoniemi and Malmi had considerably more randomness present in the gradients. The noise barrier at Itä-Pakila site might lower the pollutant levels considerably by increasing air mixing. Although the traffic pollutants near the highways seemed to vary greatly depending on meteorological conditions

1 and flow dynamics, the results obtained in this study under these environmental conditions
2 confirm that people living close to high traffic roads are generally exposed to pollutant
3 concentrations that are even double or triple of those measured at 200 m or more away from the
4 road.

5 Traffic particles in the PM₁ size fraction mostly consisted of organics and BC. The contributions
6 of traffic related organics and BC stayed rather similar during dilution of emissions (gradient
7 measurements), however, at the most open site (Pitkäjärvi) the relative concentration of
8 organics to BC increased with the distance to the highway. That additional organic mass seemed
9 to consist mostly of hydrocarbons. No evidence of the oxidation of traffic-related organics was
10 found. It was not a surprise as the oxidation of particles occurs in a much longer time period
11 than few minutes covered in this study. Additionally, the measurements were carried out in
12 autumn when solar radiation and therefore oxidant concentrations were small. Particles also
13 contained some metals. Aluminum, iron and vanadium had concentration gradients at
14 Herttoniemi and Pitkäjärvi suggesting them to originate from traffic. Zinc decreased with a
15 distance from the highway only at Herttoniemi.

16 Regarding number and volume size distributions, particle growth along the gradient was not
17 observed, the particle growth was only visible when comparing fresh emissions to background
18 conditions. However, the mass size distributions at Herttoniemi, measured with the SP-AMS,
19 showed a visible shift of the mode, detected at ~100 nm at the roadside, to a larger size when
20 the distance to roadside increased. That mode consisted mostly of rBC and hydrocarbons and
21 was found to be relatively low volatile.

22 The fleet average emission factors for particle numbers appeared to be somewhat lower than
23 those reported by Yli-Tuomi et al. (2004). Conversely, the emission factor for NO₂ showed an
24 increase. The likely reason is the increased fraction of LD diesel vehicles over the ten years.
25 The fraction of heavy duty traffic, although constituting less than 10 % of the total traffic flow,
26 was found to have a large impact on the emissions.

28 **Acknowledgements**

29 The MMEA project was supported by Tekes (the Finnish Funding Agency for Technology and
30 Innovation) and coordinated by the Finnish energy and environment cluster - CLEEN Ltd. This
31 research was also partly founded by Academy of Finland (grant no 259016), European Social

1 found (SPIRIT, contract no. P-MR-10/04) and the EUROSTARS grant E!4825 FC Aeth. I.
2 Ježek and G. Močnik are employed in Aerosol d.o.o. where the Aethalometer was developed
3 and is manufactured. The authors are very grateful to Mr. Aleksi Malinen and Mr. Kaapo
4 Lindholm Metropolia University of Applied Sciences for technical expertise and operation of
5 Sniffer.

6

1 **References**

- 2 Alföldy, B., Gieschaskiel, B., Hofmann, W., and Drossinos, Y.: Size-distribution dependent
3 lung deposition of diesel exhaust particles, *J. Aerosol Sci.*, 40, 652-663, 2009.
- 4 Arnold, F., Pirjola, L., Rönkkö, T., Reichl, U., Schlager, H., Lähde, T., Heikkilä, J., and
5 Keskinen, J.: First on-line measurements of sulfuric acid gas in modern heavy duty diesel
6 engine exhaust: Implications for nanoparticle formation, *Environ. Sci. Technol.*, 46,
7 11227–11234, 2012..
- 8 Aurela, M., Saarikoski, S., Niemi, J.V., Canonaco, F., A.S.H., Frey, A., Carbone, S., Kousa, A.
9 and Hillamo, R.: Chemical and source characterization of submicron particles at residential and
10 traffic sites in the Helsinki Metropolitan area, Finland. *Aerosol Air Qual. Res.* 15: 1213–1226,
11 2015.
- 12 Beckerman, B., Jerrett, M., Brook, J. R., Verma, D. K., Arain, M. A., Finkelstein, M. M.:
13 Correlation of nitrogen dioxide with other traffic pollutants near a major expressway, *Atmos.*
14 *Environ.* 42, 275-290, 2008.
- 15 Blum, S. A., Robert G. Bergman, R. G., Ellman, J. A.: Enantioselective Oxidation of Di-tert-
16 Butyl Disulfide with a Vanadium Catalyst: Progress toward Mechanism Elucidation, *J. Org.*
17 *Chem.*, 68 150–155, 2003.
- 18 Bowker, G.E., Baldauf, R., Isakov, V., Khlystov, A., Petersen, W.: The effects of roadside
19 structures on the transport and dispersion of ultrafine particles from highways, *Atmospheric*
20 *Environment*, 41, 8128–8139, doi.org/10.1016/j.atmosenv.2007.06.064, 2007.
- 21 CAFÉ, 2015, http://ec.europa.eu/environment/air/index_en.htm
- 22 Canagaratna, M. R., Jayne, J. T., Ghertner, D. A., Herndon, S., Shi, Q., Jimenez, J. L., Silva, P.
23 I., Williams, P., Lanni, T., Drewnick, F., Demerjian, K. L., Kolb, C. E., and Worsnop, D. R.:
24 Chase Studies of Particulate Emissions from in-use New York City Vehicles, *Aerosol Sci.*
25 *Technol.*, 38, 555–573, 2004.
- 26 Canagaratna, M. R., Jayne, J. T., Jimenez, J. L., Allan, J. D., Alfarra, M. R., Zhang, Q., Onasch,
27 T. B., Drewnick, F., Coe, H., Middlebrook, A., Delia, A., Williams, L. R., Trimborn, A. M.,
28 Northway, M. J., DeCarlo, P. F., Kolb, C. E., Davidovits, P. and Worsnop, D. R.: Chemical and
29 Microphysical Characterization of Ambient Aerosols with the Aerodyne Aerosol Mass
30 Spectrometer. *Mass Spectrom. Rev.*, 26, 185–222, 2007.

1 Canagaratna, M. R., Onasch, T. B., Wood, E.C., Herndon, S.C., Jayne, J. T., Cross, E.S., Miake-
2 Lye, R.C., Kolb, C.E., and Worsnop, D. R.: Evolution of vehicle exhaust particles in the
3 atmosphere, *J. Air & Waste Manage. Assoc.*, 60, 1192-1203, 2010.

4 Canagaratna, M. R., Jimenez, J. L., Kroll, J. H., Chen, Q., Kessler, S. H., Massoli, P.,
5 Hildebrandt Ruiz, L., Fortner, E., Williams, L. R., Wilson, K. R., Surratt, J. D., Donahue, N.
6 M., Jayne, J. T., and Worsnop, D. R.: Elemental ratio measurements of organic compounds
7 using aerosol mass spectrometry: characterization, improved calibration, and implications,
8 *Atmos. Chem. Phys.*, 15, 253–272, 2015.

9 Carbone, S., Onasch, T., Saarikoski, S., Timonen, H., Saarnio, K., Sueper, D., Rönkkö, T.,
10 Pirjola, L., Worsnop, D. & Hillamo, R.: Characterization of trace metals with the SP-AMS:
11 detection and quantification, *Atmos. Meas. Tech.*, 8, 4803-4815, 2015.

12 Carslaw, D.C., and Thys-Tyler, G.: New insights from comprehensive on-road measurements
13 of NO_x, NO₂ and NH₃ from vehicle emission remote sensing in London, UK, *Atmos. Environ.*,
14 81, 339-347, 2013.

15 Chirico, R., Prevot, A. S. H., DeCarlo, P. F., Heringa, M. F., Richter, R., Weingartner, E., and
16 Baltensperger, U.: Aerosol and trace gas vehicle emission factors measured in a tunnel using
17 an Aerosol Mass Spectrometer and other on-line instrumentation, *Atmos. Environ.*, 45, 2182-
18 2192, 2011. Clements, A. L., Jia, Y., Denbleyker, A., McDonald-Buller, E., Fraser, M. P., Allen,
19 D. T., Collins, D. R., Michel, E., Pudota, J., Sullivan, D., and Zhu, Y.: Air pollutant
20 concentrations near three Texas roadways, part II: Chemical characterization and
21 transformation of pollutants, *Atmos. Environ.*, 43, 4523-4534, 2009.

22 Dallmann, T. R., Onasch, T. B., Kirchstetter, T. W., Worton, D. R., Fortner, E. C., Herndon, S.
23 C., Wood, E. C., Franklin, J. P., Worsnop, D. R., Goldstein, A. H., and R. A. Harley, R. A.:
24 Characterization of particulate matter emissions from on-road gasoline and diesel vehicles
25 using a soot particle aerosol mass spectrometer, *Atmos. Chem. Phys.*, 14, 7585–7599, 2014.

26 DeCarlo, P. F., Kimmel, J. R., Trimborn, A., Northway, M. J., Jayne, J. T., Aiken, A. C., Gonin,
27 M., Fuhrer, K., Horvath, T., Docherty, K. S., Worsnop, D. R., and Jimenez, J. L.: Field-
28 deployable, high-resolution, time-of-flight mass spectrometer, *Anal. Chem.*, 78, 8281–8289,
29 2006.

30 Durant, J. L., Ash, C. S., Wood, E. C., Herndon, S. C., Jayne, J. T., Knighton, W. B.,
31 Canagaratna, M. R., Trull, J. B., Drugge, D., Zamore, W., and Kolb, C. E.: Short-term variation

1 in near-highway air pollutant gradients on a winter morning, *Atmos. Chem. Phys.*, 10, 8341–
2 8352, doi:10.5194/acp-10-8341-2010, 2010.

3 Drinovec, L., Močnik, G., Zotter, P., Prévôt, A. S. H., Ruckstuhl, C., Coz, E., Rupakheti, M.,
4 Sciare, J., Müller, T., Wiedensohler, A., and Hansen, A. D. A.: The “dual-spot” Aethalometer:
5 an improved measurement of aerosol black carbon with realtime loading compensation, *Atmos.*
6 *Meas. Tech.*, 8, 1965–1979, doi:10.5194/amt-8-1965-2015, 2015.

7 Finnish Transport Agency: Finnish road statistics [e-publication]. Finnish Transport Agency.
8 [referred 29.12.2014]. Access method:
9 [http://portal.liikennevirasto.fi/sivu/www/f/aineistopalvelut/tilastot/tietilastot/liikennemaarakar](http://portal.liikennevirasto.fi/sivu/www/f/aineistopalvelut/tilastot/tietilastot/liikennemaarakartat#.VLUnmnv-ZKo)
10 [tat#.VLUnmnv-ZKo](http://portal.liikennevirasto.fi/sivu/www/f/aineistopalvelut/tilastot/tietilastot/liikennemaarakartat#.VLUnmnv-ZKo), 2014.

11 EEA Report No 5, <http://www.eea.europa.eu/publications/air-quality-in-europe-2015>, 2015.

12 Gilbert, N. L., Goldberg, M. S., Brook, J. R., and Jerrett, M.: The influence of highway traffic
13 on ambient nitrogen dioxide concentrations beyond the immediate vicinity of highways, *Atmos.*
14 *Environ.* 41, 2670–2673, 2007.

15 Gramotnev, G. and Ristovski, Z.: Experimental investigation of ultra-fine particle size
16 distribution near a busy road, *Atmos. Environ.*, 38, 1767–1776, 2004.

17 Hagler, G. S. W, Baldauf, R. W., Thoma, E. D., Long, T. R., Snow, R. F., Kinsey, J. S.,
18 Oudejans, L., and Gullet, B. K.: Ultrafine particles near a major roadway in Raleigh, North
19 Carolina: Downwind attenuation and correlation with traffic-related pollutants, *Atmos.*
20 *Environ.*, 43, 1229-1234, 2009.

21 Heikkilä, J., Rönkkö, T., Lähde, T., Lemmetty, M., Arffman, A., Virtanen, A., Keskinen, J.,
22 Pirjola, L., and Rothe, D.: Effect of open channel filter on particle emissions of modern diesel
23 engine, *J. Air & Waste Manage. Assoc.*, 59, 1148-1154, DOI:10.3155/1047-3289.59.10.1148,
24 2009.

25 IPCC: Climate Change 2013, The Physical Science Basis, Working Group I, Switzerland,
26 https://www.ipcc.ch/pdf/assessment-report/ar5/wg1/WGIAR5_SPM_brochure_en.pdf.

27 Janhäll, S.: Review on urban vegetation and particle air pollution - Deposition and dispersion,
28 *Atmos. Environ.*, 105, 130-137, 2015.

29 Ježek, I., Katrašnik, T., Westerdahl, D., and Močnik, G.: Black carbon, particle number
30 concentration and nitrogen oxide emission factors of random in-use vehicles measured with the

1 on-road chasing method, *Atmos. Chem. Phys.*, 15, 11011–11026, doi:10.5194/acp-15-11011-
2 2015, 2015.

3 Johansson, C., Norman, M., and Gidhagen, L.: Spatial & temporal variations of PM₁₀ and
4 particle number concentrations in urban air, *Environ. Monit. Assess.*, 127, 477–487, 2007. Karl,
5 M., Kukkonen, J., Keuken, M.P., Lützenkirchen, S., Pirjola, L., and Hussein, T.: Modelling and
6 Measurements of Urban Aerosol Processes on the Neighbourhood Scale in Rotterdam, Oslo
7 and Helsinki, *Atmos. Chem. Phys. Discuss.*, 15, 35157–35200, 2015

8 Keskinen, J., Pietarinen, K., and Lehtimäki, M.: Electrical Low Pressure Impactor, *J. Aerosol*
9 *Sci.*, 23, 353–360, 1992.

10 Kettunen, J., Lanki, T., Tiittanen, P., Aalto, P. P., Koskentalo, T., Kulmala, M., Salomaa, V.,
11 and Pekkanen, J.: Associations of fine and ultrafine particulate air pollution with stroke
12 mortality in an area of low air pollution levels, *Stroke*, 38, 918–922, 2007.

13 Kittelson, D.B.: Engines and nano-particles: a review, *J. Aerosol Sci.*, 29, 575–588, 1998.

14 Kittelson, D. B., Watts, W. F., Johnson, J. P., Thorne, C., Higham, C., Payne, J., Goodier, S.,
15 Warrens, C., Preston, H., Zink, U., Pickles, D., Goersmann, C., Twigg, M. V., Walker, A. P.,
16 and Boddy, R.: Effect of fuel and lube oil sulfur on the performance of a diesel exhaust gas
17 continuously regenerating trap, *Environ. Sci. Technol.*, 42, 9276–9282, 2008.

18 Kristensson, A., Johansson, C., Westerholm, R., Swietlicki, E., Gidhagen, L., Wideqvist, U.,
19 and Vesely, V.: Real-world traffic emission factors of gases and particles measured in a road
20 tunnel in Stockholm, Sweden, *Atmos. Environ.*, 38, 657–673, 2004.

21 Kumar, P., Robins, A., Vardoulakis, S., and Britter, R.: A review of the characteristics of
22 nanoparticles in the urban atmosphere and the prospects for developing regulatory controls,
23 *Atmos. Environ.*, 44, 5035–5052, 2010.

24 Lee, A. K. Y., Willis, M. D., Healy, R. M., Onasch, T. B., and Abbatt, J. P. D.: Mixing state
25 of carbonaceous aerosol in an urban environment: single particle characterization using the
26 soot particle aerosol mass spectrometer (SP-AMS), *Atmos. Chem. Phys.*, 15, 1823–1841,
27 2015.

28 Lähde, T., Niemi, J.V., Kousa, A., Rönkkö, T., Karjalainen, P., Keskinen, J., Frey, A., Hillamo,
29 R., and Pirjola, L.: Mobile Particle and NO_x Emission Characterization at Helsinki Downtown:
30 Comparison of Different Traffic Flow Areas, *Aerosol Air Qual. Res.*, 14, 1372–1382, 2014.

1 Marjamäki, M., Ntziachristos, L., Virtanen, A., Ristimäki, J. and Keskinen, J.: Electrical Filter
2 Stage for the ELPI, SAE Technical Paper 2002-01-0055, 2002.

3 Massoli, P., Fortner, E.C., Canagaratna, M. R., Williams, L. R., Zhang, Q., Sun, Y., Schwab, J.
4 J., Trimborn, A., Onasch, T. B., Demerjian, K. L., Kolb, C. E., Worsnop, D. R., and Jayne, J.
5 T.: Pollution Gradients and Chemical Characterization of Particulate Matter from Vehicular
6 Traffic near Major Roadways: Results from the 2009 Queens College Air Quality Study in
7 NYC, *Aerosol Sci. Technol.*, 46, 1201-1218, DOI: 10.1080/02786826.2012.701784, 2012.

8 Morawska, L., Ristovski, Z., Jayaratne, E. R., Koegh, D. U., and Ling, X.: Ambient nano and
9 ultrafine particles from motor vehicle emissions: Characteristics, ambient processing and
10 implications on human exposure, *Atmos. Environ.*, 42, 8113–8138, 2008.

11 Ning, Z., Hudda, N., Daher, N., Kam, W., Herner, J., Kozawa, K., Mara, S., and Sioutas, D.:
12 Impact of roadside noise barriers on particle size distributions and pollutants concentrations
13 near freeways, *Atmos. Environ.*, 44, 3118-3127, 2010.

14 Official Statistics of Finland: Motor vehicle stock [e-publication]. Helsinki: Advisory Board of
15 OSF [referred 28.11.2014]. Access method:
16 http://pxweb2.stat.fi/database/StatFin/lii/mkan/mkan_en.asp.

17 Onasch, T. B., Trimborn, A., Fortner, E. C., Jayne, J. T., Kok, G. L., Williams, L. R.,
18 Davidovits, P., and Worsnop, D. R.: Soot Particle Aerosol Mass Spectrometer: Development,
19 Validation, and Initial Application, *Aerosol Sci. Technol.*, 46, 804–817, 2012.

20 Padró-Martinez, L. T., Patton, A. P., Trull, J. B., Zamore, W., Brugge, D., and Durant, J. L.:
21 Mobile monitoring of particle number concentration and other traffic-related air pollutants in a
22 near-highway neighborhood over the course of a year, *Atmos. Environ.*, 61, 253-264, 2012.

23 Pey, J., Querol, X., Alastuey, A., Rodriguez, S., Putaud, J. P., and Van Dingenen, R.: Source
24 apportionment of urban fine and ultrafine particle number concentration in a Western
25 Mediterranean city, *Atmos. Environ.*, 43, 4407–4415, 2009.

26 Pirjola, L., Parviainen, H., Hussein, T., Valli, A., Hämeri, K., Aalto, P., Virtanen, A., Keskinen,
27 J., Pakkanen, T., Mäkelä, T. and Hillamo, R.: “Sniffer” – A Novel Tool for Chasing Vehicles
28 and Measuring Traffic Pollutants. *Atmos. Environ.*, 38: 3625–3635, 2004.

29 Pirjola, L., Paasonen, P., Pfeiffer, D., Hussein, T., Hämeri, K., Koskentalo, T., Virtanen, A.,
30 Rönkkö, T., Keskinen, J., Pakkanen, T. A., and Hillamo, R. E.: Dispersion of particles and trace

1 gases nearby a city highway: Mobile laboratory measurements in Finland, *Atmos. Environ.*, 40,
2 867-879, 2006.

3 Pirjola, L., Lähde, T., Niemi, J.V., Kousa, A., Rönkkö, T., Karjalainen, P., Keskinen, J., Frey,
4 A., Hillamo, R.: Spatial and temporal characterization of traffic emission in urban
5 microenvironments with a mobile laboratory, *Atmos. Environ.*, 63, 156-167, 2012.

6 Pirjola, L., Dittrich, A., Niemi, J. V., Saarikoski, S., Timonen, H., Kuuluvainen, H., Järvinen,
7 A., Kousa, A., Rönkkö, T., and Hillamo, R.: Physical and chemical characterization of real-
8 world particle number and mass emissions from city buses in Finland, *Environ. Sci. Technol.*,
9 50, 294-304, 2016.

10 Pope, C.A., III, and Dockery, D.W.: Health effects of fine particulate air pollution: Lines that
11 connect, *J. Air Waste Manage. Assoc.*, 56, 707-742, 2006.

12 Robinson, A. L., Grieshop, A. P., Donahue, N. M., and Hunt, S.W.: Updating the conceptual
13 model for fine particle mass emissions from combustion systems, *J. AirWaste Manage.*, 60,
14 1204–1222, 2010.

15 Rönkkö, T., Arffman, A., Karjalainen, P., Lähde, T., Heikkilä, J., Pirjola, L., Rothe, D., and
16 Keskinen, J.: Diesel exhaust nanoparticle volatility studies by a new thermodenuder with low
17 solid nanoparticle losses, Abstracts in the 15th ETH-Conference on Combustion Generated
18 Nanoparticles, 26–29 June 2011, Zürich, Switzerland, 2011.

19 Rönkkö, T., Lähde, T., Heikkilä, J., Pirjola, L., Bauschke, U., Arnold, F. , Schlager, 472 H.,
20 Rothe, D., Yli-Ojanperä, J., and Keskinen, J.: Effect of gaseous sulphuric acid on diesel exhaust
21 nanoparticle formation and characteristics, *Environ. Sci. Technol.*, 47, 474 11882-11889,
22 [dx.doi.org/10.1021/es402354y](https://doi.org/10.1021/es402354y), 2013.

23 Saarikoski, S., Frey, A., Mäkelä, T., and Hillamo, R.: Size distribution measurement of
24 carbonaceous particulate matter using a low pressure impactor with quartz fiber substrates,
25 *Aerosol Sci. Technol.*, 42, 603–612, 2008.

26 Salcedo, D., Onasch, T. B., Aiken, A. C., Williams, L. R., de Foy, B., Cubison, M. J., Worsnop,
27 D. R., Molina, L. T., and Jimenez, J. L.: Determination of particulate lead using aerosol mass
28 spectrometry: MILAGRO/MCMA-2006 observations, *Atmos. Chem. Phys.*, 10, 5371–5389,
29 [doi:10.5194/acp-10-5371-2010](https://doi.org/10.5194/acp-10-5371-2010), 2010.

1 Salcedo, D., Laskin, A., Shutthanandan, V., and Jimenez, J.-L.: Feasibility of the Detection of
2 Trace Elements in Particulate Matter Using Online High-Resolution Aerosol Mass
3 Spectrometry, *Aerosol Sci. Technol.*, 46, 1187–1200, 2012.

4 Schneider, J., Kirchner, U., Borrmann, S., Vogt, R., Scheer, V.: In situ measurements of particle
5 number concentration, chemically resolved size distributions and black carbon content of
6 traffic-related emissions on German motorway, rural roads and in city traffic, *Atmos. Environ.*,
7 42, 4257-4268, 2008.

8 Sharma, A., Massey, D. D., and Taneja, A.: Horizontal gradients of traffic related air pollutants
9 near a major highway in Agra, India, *Indian Journal of Radio & Space Physics*, 38, 338-346,
10 2009

11 Shields, L. G., Suess, D. T., and Prather, K. A.: Determination of single particle mass spectral
12 signatures from heavy-duty diesel vehicle emissions for PM_{2.5} source apportionment, *Atmos.*
13 *Environ.*, 41, 3841-3852, 2007.

14 Sioutas, C., Delfino, R. J., and Singh, M.: Exposure assessment for atmospheric ultrafine
15 particles (UFPs) and implications in epidemiologic research, *Environ. Health Perspect.*, 113,
16 947–955, 2005.

17 Sodeman, D. A., Toner, S.M., and Prather, K. A.; Determination of single particle mass spectral
18 signatures from light-duty vehicle emissions, *Environ. Sci. Technol.*, 39, 4569-4580, 2005.

19 Su, D. S., Serafino, A., Müller, J.-O., Jentoft, R. E., Schlögl, R., Fiorito, S. Cytotoxicity and
20 Inflammatory Potential of Soot Particles of Low-Emission Diesel Engines, *Environ. Sci.*
21 *Technol.*, 42, 1761–1765, 2008.

22 Tobias, H. J., Beving, D. E., Ziemann, P.J., Sakurai, H., Zuk, M., McMurry, P.H., Zarling, D.,
23 Waytulonis, R., and Kittelson, D.B.: Chemical analysis of diesel engine nanoparticles using a
24 nano-DMA/thermal desorption particle beam mass spectrometer. *Environ Sci Technol.* 35,
25 2233-2243, doi:10.1021/es0016654, 2001.

26 Wang, F., Ketzel, M., Ellermann, T., Wahlin, P., Jensen, S. S., Fang, D., and Massling, A.:
27 Particle number, particle mass and NO_x emission factors at a highway and an urban street in
28 Copenhagen, *Atmos. Chem. Phys.*, 10, 2745–2764, 2010.

1 Weilenmann, M., Favez, J.-Y., and Alvarez, R.: Cold-start emissions of modern passenger cars
2 at different low ambient temperatures and their evolution over vehicle legislation categories,
3 *Atmos. Environ.*, 43, 2419–2429, 2009.

4 Westerdahl, D., Wang, X., Pan, X., and Zhang, K.M.: Characterization of on-road vehicle
5 emission factors and microenvironmental air quality in Beijing, China. *Atmos. Environ.*, 43,
6 697–705, 2009.

7 Worton, D., Isaacman, G., Gentner, D.R., Dallmann, T. R., Chan, A.W. H., Ruehl, C.,
8 Kirchstetter, T. W., Wilson, K. R., Harley, R. A., and Goldstein, A. H.: Lubricating Oil
9 Dominates Primary Organic Aerosol Emissions from Motor Vehicles, *Environ. Sci. Technol.*,
10 48, 3698–3706, [dx.doi.org/10.1021/es405375j](https://doi.org/10.1021/es405375j), 2014.

11 Yli-Ojanperä, J., Kannosto, J., Marjamäki, M. and Keskinen, J.: Improving the Nanoparticle
12 Resolution of the ELPI. *Aerosol Air Qual. Res.*, 10, 360–366, 2010.

13 Yli-Tuomi, T., Aarnio, P., Pirjola, L., Mäkelä, T., Hillamo, R., and Jantunen, M.: Emissions of
14 fine particles, NO_x and CO from onroad vehicles in Finland, *Atmos. Environ.*, 39, 6696–6706,
15 2004.

16 Zhu, Y.F., Hinds, W.C., Kim, S., and Sioutas, C.: Concentration and size distribution of ultrafine
17 particles near a major highway, *Air & Waste Manage. Assoc.*, 52, 1032–1042, 2002.

18 Zhu, Y., Pudota, J., Collins, D., Allen, D., Clements, A., DenBleyker, A., Fraser, M., Jia, Y.,
19 McDonald-Buller, E., and Michel, E.: Air pollutant concentrations near three Texas roadways,
20 Part I: Ultrafine particles. *Atmos. Environ.*, 43, 4513–4522, 2009.

21

Table 1. Average of hourly meteorological conditions as recorded by the HSY at the Ämmässuo site, representing the regional air mass properties. The traffic LD and HD data are based on the manual three minute observations, and the annual mean traffic flow per day by the Finnish Transport Agency.

| Site | T °C | RH % | Wind direction ° | Wind speed m/s | Traffic LD veh/h | Traffic HD veh/h | % of HD | Annual mean (veh/day) |
|-------------|---------------|--------------|------------------------|----------------------|------------------------|------------------------|------------|-----------------------------|
| Pitkäjärvi | 1.8 ± 2.3 | 83 ± 12 | 326 ± 30 | 2.7 ± 1.7 | 3400 | 320 | 8.7 | 40000 |
| Malmi | 3.1 ± 1.9 | 84 ± 5.8 | 155 ± 23 | 4.6 ± 1.2 | 4400 | 230 | 4.8 | 55000 |
| Itä-Pakila | 4.7 ± 2.0 | 89 ± 7.0 | 143 ± 10 | 4.4 ± 0.8 | 5900 | 160 | 2.8 | 57000 |
| Herttoniemi | 0.8 ± 2.8 | 77 ± 13 | 257 ± 30 | 2.4 ± 1.1 | 3900 | 110 | 2.9 | 50000 |

1 Table 2. Mean pollutant concentrations along with standard deviations (std) at the highway
2 (HW), roadside (RS) and background (BG) at the four sites. The distance from the curb to the
3 exact measurement location is indicated in the brackets following RS. CN was measured by the
4 CPC, BC by the aethalometer and Org, NO₃, SO₄ and NH₄ by the SP-AMS.

| | Herttoniemi | | | Malmi | | | Itä-Pakila | | | Pitkäjärvi | | |
|--|-------------|--------------|-------|-------|--------------|------|------------|------------|------|------------|--------------|------|
| | HW | RS (11 m) | BG | HW | RS (11 m) | BG | HW | RS (6m) | BG | HW | RS (14 m) | BG |
| CN | 7.72 | 4.23 | 0.71 | 8.60 | 10.8 | 1.09 | 8.63 | 5.22 | 1.00 | 12.3 | 10.3 | 0.89 |
| std (x10 ⁴ cm ⁻³) | 9.05 | 4.41 | 0.20 | 9.86 | 7.28 | 0.20 | 9.68 | 4.60 | 0.36 | 13.9 | 6.1 | 0.92 |
| PM ₁ | 11.2 | 8.64 | 2.22 | 17.1 | 12.5 | 6.69 | 16.8 | 9.97 | 7.02 | 10.9 | 7.52 | 2.19 |
| std (µg m ⁻³) | 10.9 | 6.15 | 0.51 | 17.1 | 5.73 | 1.61 | 14.6 | 3.54 | 1.43 | 7.15 | 3.49 | 0.87 |
| BC | 6.08 | 4.95 | 0.57 | 6.84 | 4.26 | 0.63 | 4.68 | 2.99 | 0.65 | 4.45 | 3.52 | 0.43 |
| std (µg m ⁻³) | 9.29 | 5.99 | 0.27 | 12.8 | 3.23 | 0.30 | 5.34 | 1.93 | 0.31 | 5.02 | 1.96 | 0.30 |
| Org | 4.55 | 3.22 | 1.33 | 7.83 | 6.01 | 3.37 | 9.01 | 4.56 | 3.62 | 5.54 | 3.36 | 0.97 |
| std (µg m ⁻³) | 5.72 | 1.38 | 0.43 | 11.3 | 4.61 | 1.15 | 13.6 | 2.80 | 1.00 | 5.07 | 2.88 | 0.73 |
| NO ₃ | 0.09 | 0.10 | 0.08 | 0.58 | 0.62 | 0.73 | 0.91 | 0.88 | 0.94 | 0.19 | 0.13 | 0.11 |
| std (µg m ⁻³) | 0.05 | 0.07 | 0.04 | 0.40 | 0.43 | 0.50 | 0.70 | 0.90 | 0.93 | 0.19 | 0.13 | 0.12 |
| SO ₄ | 0.36 | 0.29 | 0.18 | 1.30 | 1.10 | 1.40 | 1.50 | 1.00 | 1.20 | 0.57 | 0.38 | 0.53 |
| std (µg m ⁻³) | 0.23 | 0.20 | 0.06 | 1.10 | 0.88 | 0.88 | 0.03 | 0.26 | 0.07 | 0.32 | 0.22 | 0.34 |
| NH ₄ | 0.10 | 0.09 | 0.06 | 0.51 | 0.50 | 0.56 | 0.68 | 0.54 | 0.61 | 0.20 | 0.13 | 0.15 |
| std (µg m ⁻³) | 0.08 | 0.08 | 0.003 | 0.40 | 0.38 | 0.38 | 0.21 | 0.33 | 0.27 | 0.12 | 0.01 | 0.10 |
| NO | 132 | 52.4 | 0.4 | 150 | 107 | 2.00 | 94.5 | 65.4 | 3.10 | 138 | 105 | 7.40 |
| std (µg m ⁻³) | 146 | 48.6 | 0.80 | 348 | 69.5 | 0.90 | 95.8 | 43.4 | 1.9 | 142 | 57.6 | 32.3 |
| NO ₂ | 73.0 | 46.0 | 12.3 | 54.2 | 76.6 | 18.0 | 61.4 | 50.7 | 19.2 | 54.3 | 62.1 | 15.3 |
| std (µg m ⁻³) | 89.6 | 27.4 | 3.30 | 284 | 39.2 | 5.60 | 57.9 | 30.3 | 7.60 | 75.2 | 33.3 | 41.0 |
| NO _x | 205 | 98.4 | 12.6 | 204 | 184 | 20.0 | 156 | 116 | 22.3 | 192 | 167 | 22.7 |
| std (µg m ⁻³) | 190 | 70.5 | 3.30 | 304 | 97.0 | 5.90 | 125 | 59.0 | 8.80 | 176 | 78.8 | 67.7 |

5

6

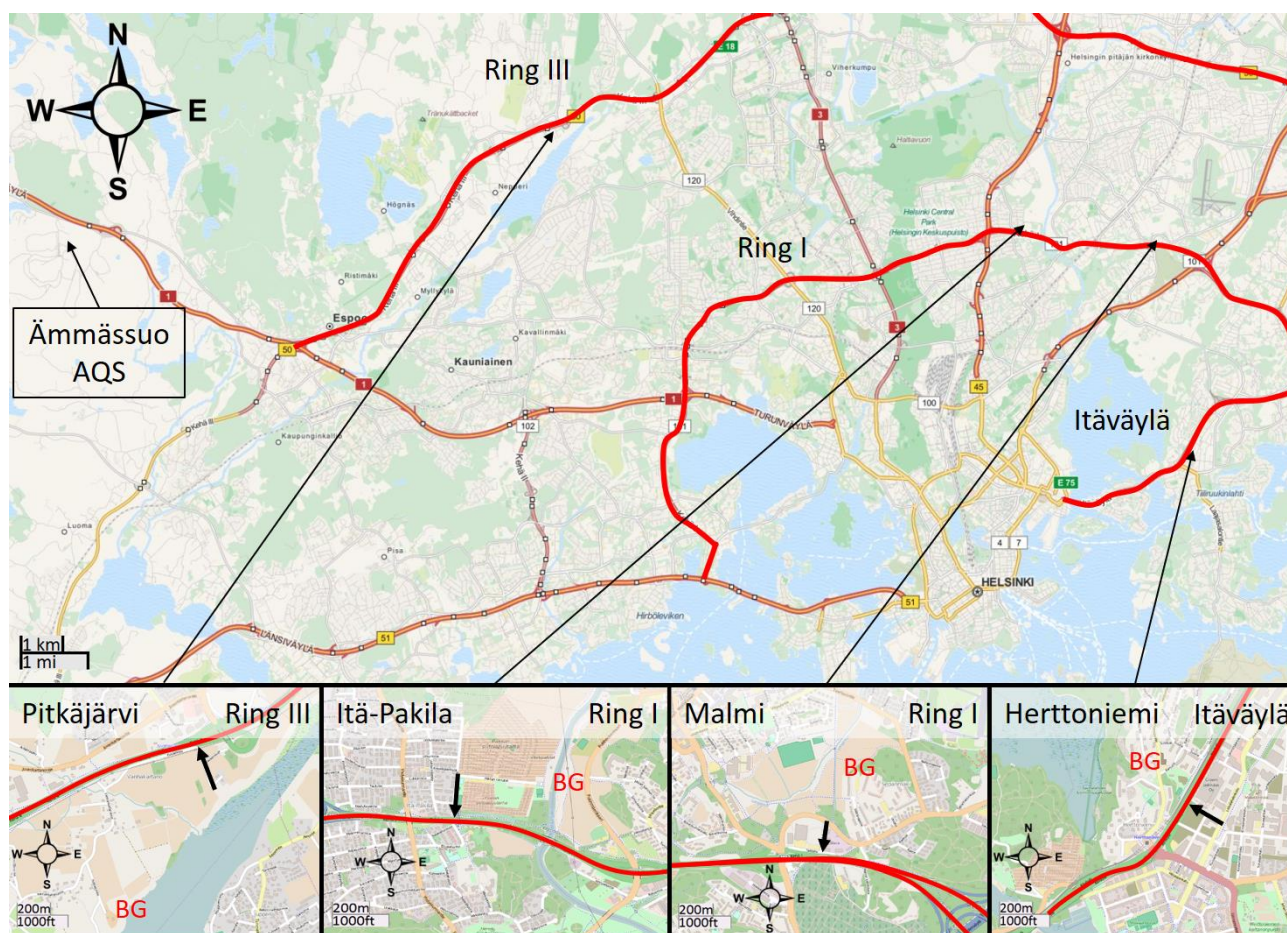
1 Table 3. Average emission factors along with standard deviations calculated from the
2 measurements on the highways.

| | | Herttoniemi | Malmi | Itä-Pakila | Pitkäjärvi |
|--|------|-----------------------|-----------------------|-----------------------|------------------------|
| EF _{CN} (# (kg fuel) ⁻¹) | Mean | 4.9x10 ¹⁵ | 6.1 x10 ¹⁵ | 6.5 x10 ¹⁵ | 11.6 x10 ¹⁵ |
| | Std | 6.5 x10 ¹⁵ | 5.7 x10 ¹⁵ | 7.1 x10 ¹⁵ | 14.6 x10 ¹⁵ |
| EF _{PM1} (g (kg fuel) ⁻¹) | Mean | 0.78 | 1.17 | 0.99 | 0.39 |
| | Std | 0.74 | 1.87 | 2.09 | 1.29 |
| EF _{BC} (g (kg fuel) ⁻¹) | Mean | 0.43 | 0.54 | 0.30 | 0.15 |
| | Std | 0.67 | 0.65 | 0.22 | 1.14 |
| EF _{Org} (g (kg fuel) ⁻¹) | Mean | 0.26 | 0.33 | 0.33 | 0.24 |
| | Std | 0.33 | 0.20 | 0.17 | 0.13 |
| EF _{NO} (g (kg fuel) ⁻¹) | Mean | 8.12 | 9.86 | 7.44 | 11.48 |
| | Std | 6.31 | 9.65 | 5.28 | 7.60 |
| EF _{NO2} (g (kg fuel) ⁻¹) | Mean | 4.14 | 4.02 | 3.45 | 4.47 |
| | Std | 4.44 | 7.26 | 3.95 | 5.79 |
| EF _{NOx} (g (kg fuel) ⁻¹) | Mean | 12.2 | 14.1 | 10.9 | 16.5 |
| | std | 8.0 | 12.2 | 6.8 | 11.8 |

3

4

1



2

3 Figure 1. Four gradient measurement locations in the Helsinki region. In the subplots, the black
 4 arrows show the driving direction on the gradient roads and BG depicts the local background
 5 measurement sites. Also shown is a meteorological measurement site at Ammässuo.
 6 (OpenStreetMap)

7

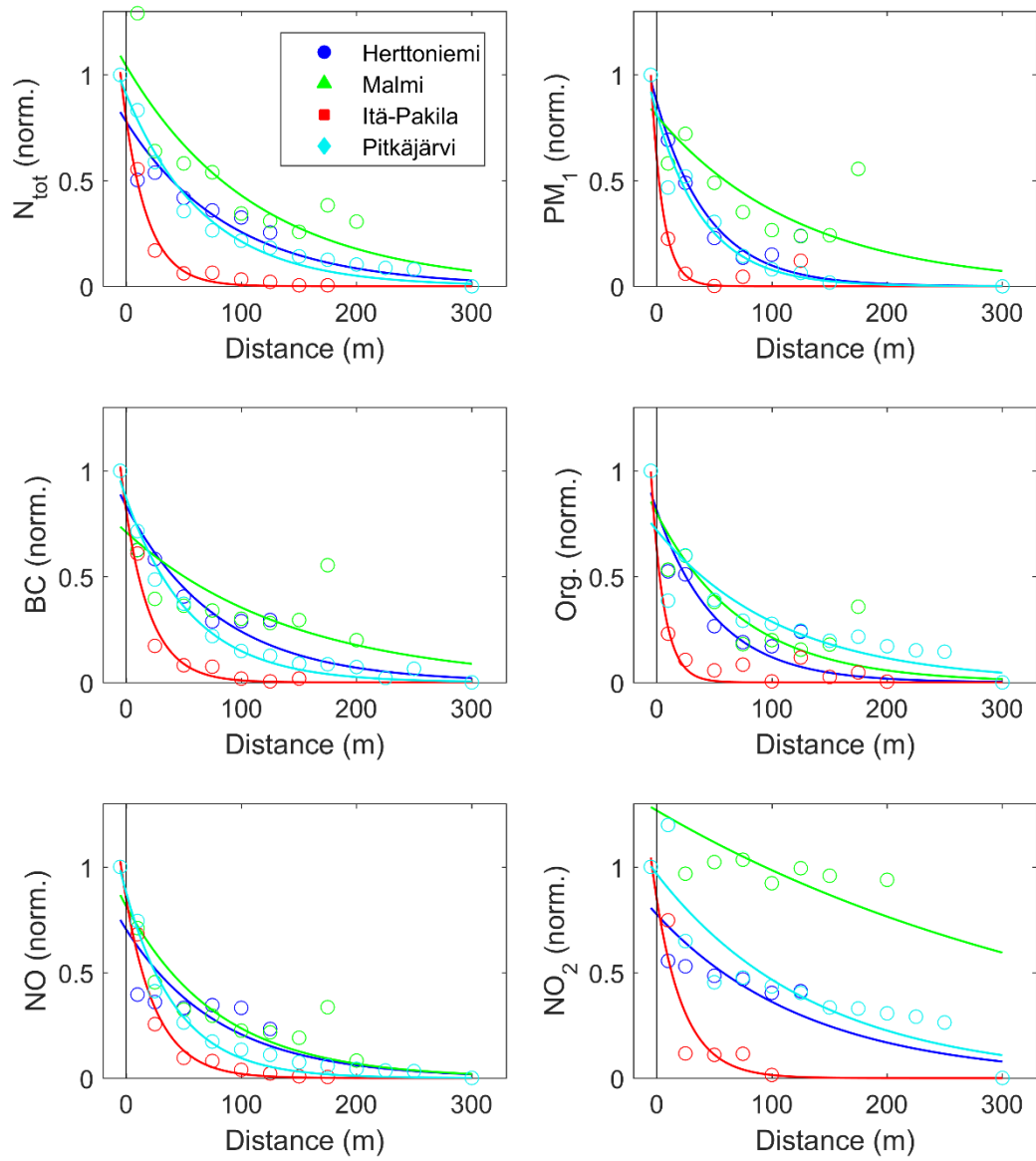
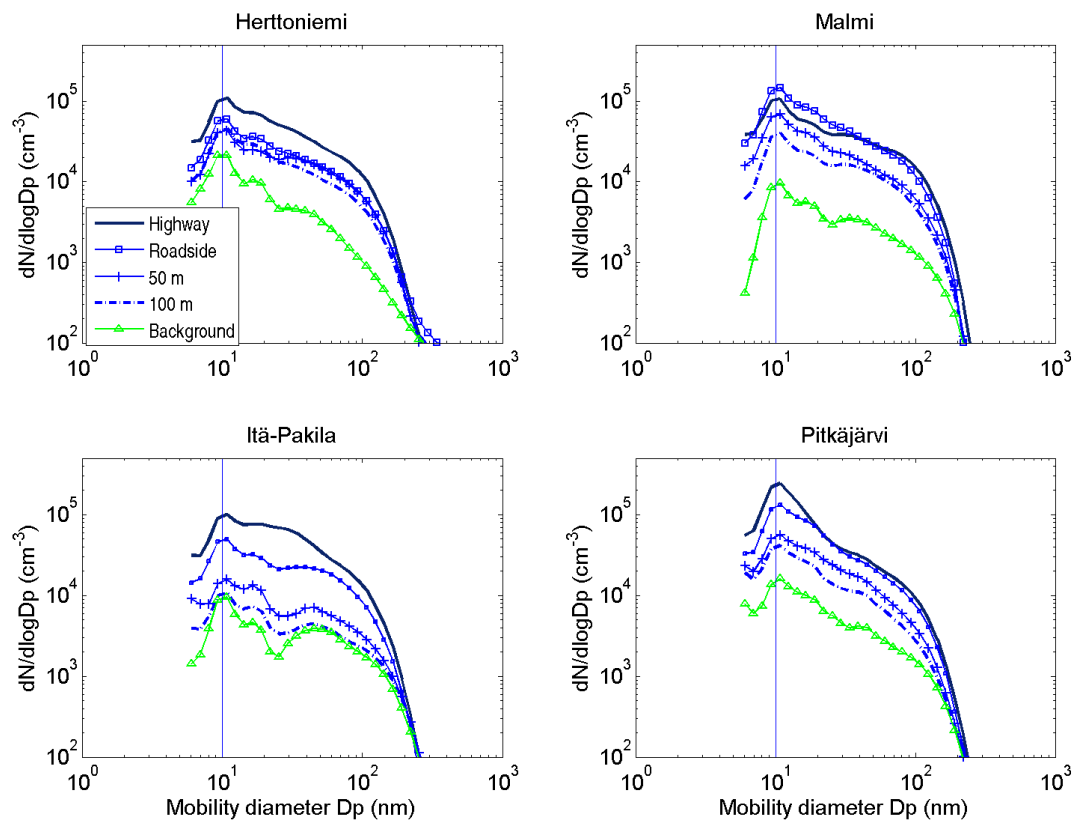


Figure 2. Normalized particle number (N_{tot}) and mass concentration (PM_{10}), BC and organics concentration, as well as NO and NO_2 concentration as a function of distance from the highway at four measurement locations shown in the legend. Zero distance refers to the edge of the road, and negative values to driving on the highway. Also shown are the fitted reduction curves. Background values were subtracted from the measured concentrations.



1

2 Figure 3. Particle size distribution as measured by the EEPS at different distances from the
 3 roadside on the four locations.

4

5

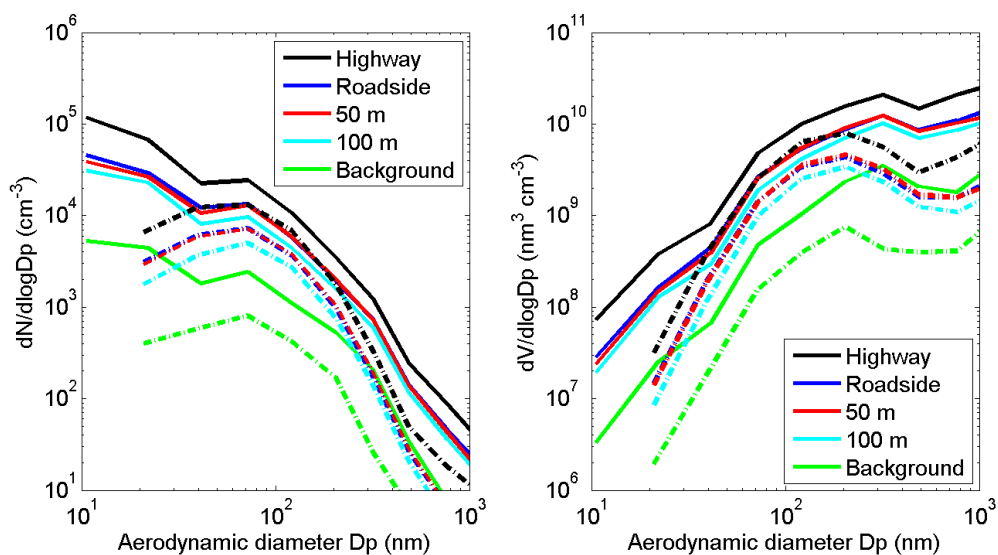


Figure 4. Average particle number size distribution (left) and volume size distribution (right) measured at different distances from the highway at Herttoniemi with two ELPIs, one measured before (solid lines) and the other after (dash dot lines) the thermodenuder. Note that x-axis refers to aerodynamic diameter.

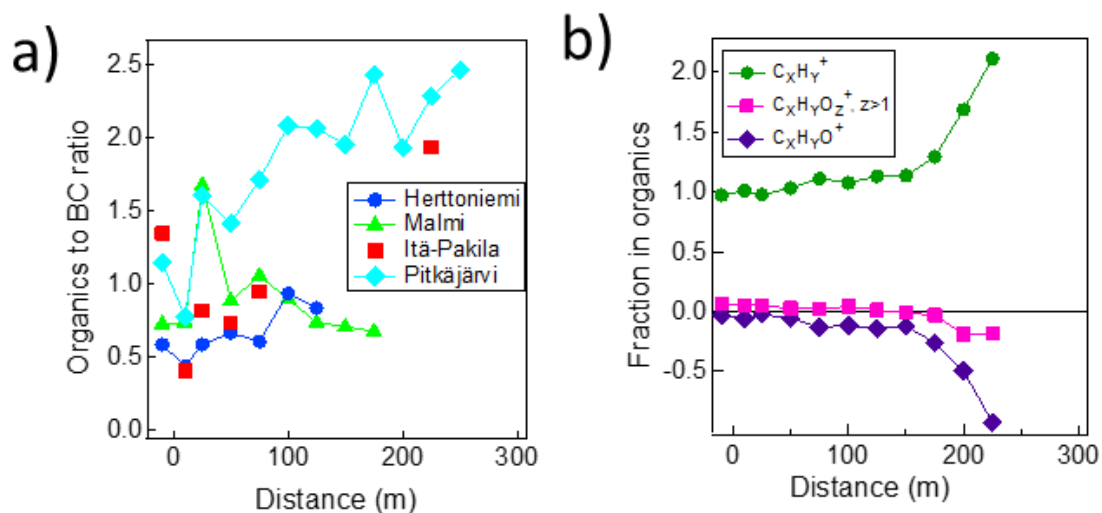


Figure 5. The average ratio of organics to BC at four sites (a) and the fractions of hydrocarbon fragments ($C_xH_y^+$) and oxidized organic fragments ($C_xH_yO^+$ and $C_xH_yO_z^+, z>1$) at Pitkäjärvi (b) as a function of the distance from the highway. Zero distance refers to the roadside and negative value driving on the highway. Background values were subtracted from the measured concentrations before calculating the ratios.

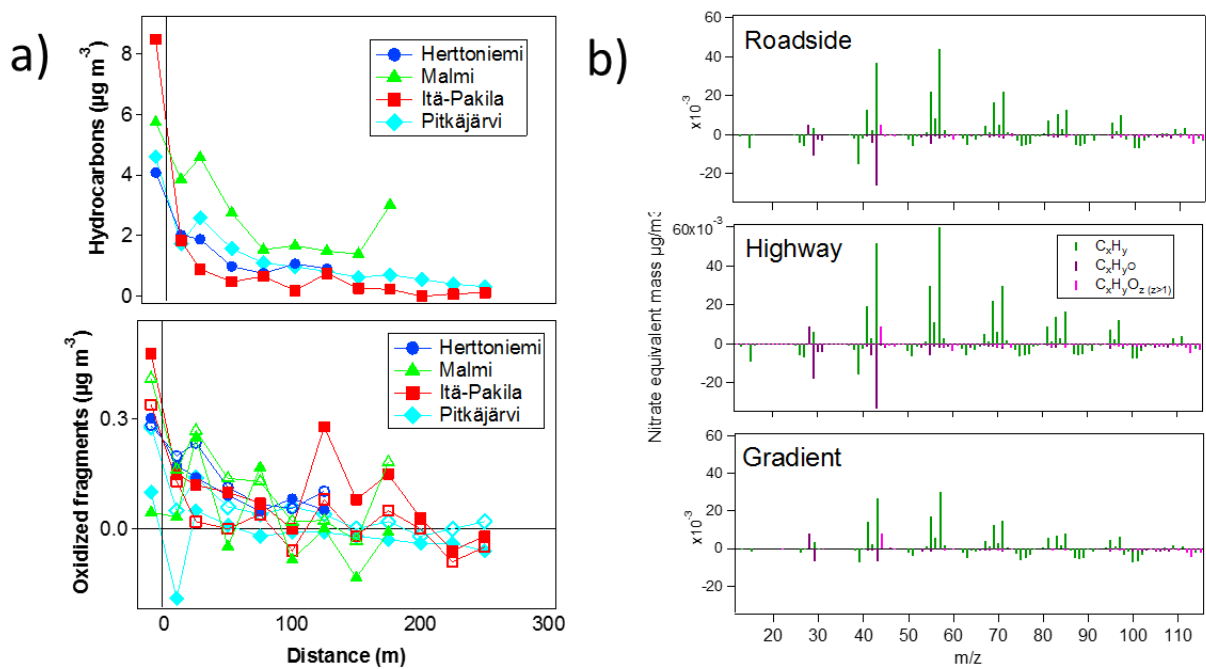
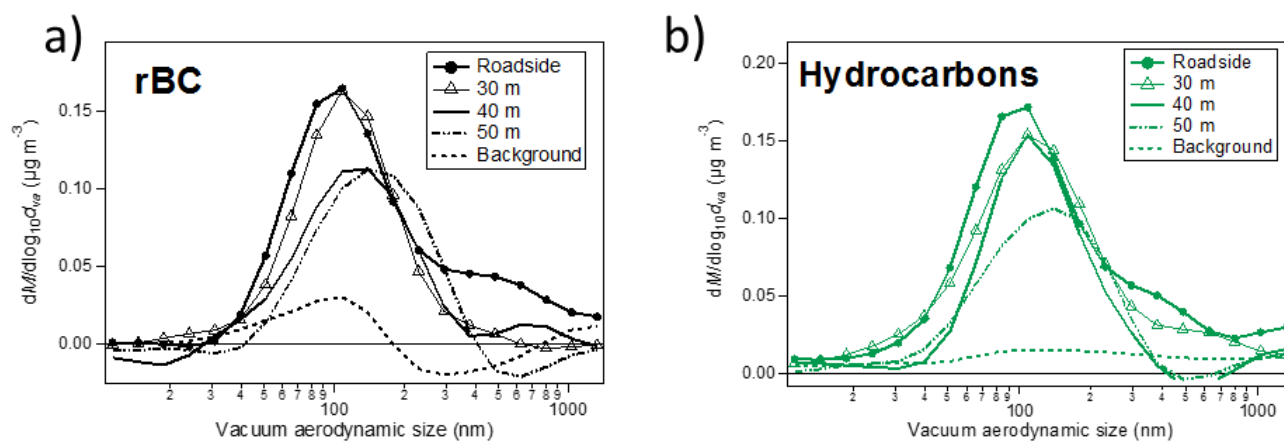


Figure 6. Concentrations of hydrocarbon fragments (C_xH_y^+) and oxidized organic fragments ($\text{C}_x\text{H}_y\text{O}^+$ and $\text{C}_x\text{H}_y\text{O}_z^+$, $z \geq 1$) measured at the four sites (a), and the average mass spectra for highway, roadside and gradient at Pitkajärvi (b). Solid markers refer to organic fragments with one oxygen atom and open markers to organic fragments with more than one oxygen atoms in lower figure of (a). In (a) zero distance refers to the roadside and negative value driving on the highway. Background values were subtracted both from the measured concentrations and mass spectra.

1



2

3 Figure 7. Particle mass size distribution at Herttoniemi on 26th of Oct 2012. m/z 36 was used
 4 as a surrogate for rBC and m/z 57 for for hydrocarbons.

5

6

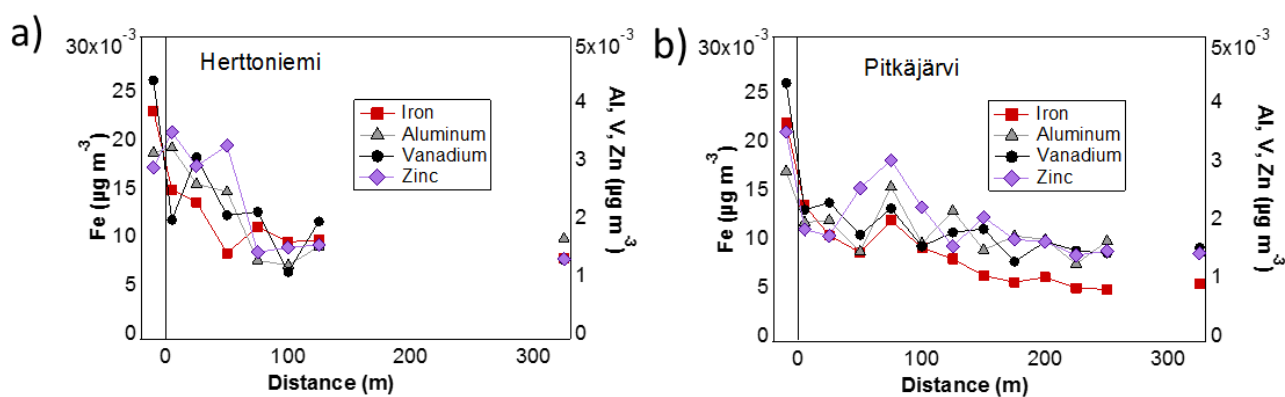


Figure 8. Concentrations of iron, aluminum, vanadium and zinc at Herttoniemi (a) and Pitkäjärvi (b) as a function of the distance from the highway. Zero distance refers to the roadside, negative values to driving on the highway and right-most point to the background location. Background values are not subtracted from the measured concentrations. Gradients for Itä-Pakila and Malmi are presented in supplement. Concentrations of metals were calculated by using the RIEs given in Carbone et al. (2015).